# Finding spectral gaps in quasicrystals

Paul Hege [1,2] Massimo Moscolari [1] and Stefan Teufel [1]
[1]*Mathematisches Institut, University of Tübingen, Auf der Morgenstelle 10, 72076 Tübingen, Germany*
[2]*Department of Neural Dynamics and MEG, Hertie Institute for Clinical Brain Research, University of Tübingen, Otfried-Müller-Str. 25, 72076 Tübingen, Germany*

(Received 30 May 2022; accepted 26 August 2022; published 21 October 2022)

We present an algorithm for reliably and systematically proving the existence of spectral gaps in Hamiltonians with quasicrystalline order, based on numerical calculations on finite domains. We apply this algorithm to prove that the Hofstadter model on the Ammann-Beenker tiling of the plane has spectral gaps at certain energies, and we are able to prove the existence of a spectral gap where previous numerical results were inconclusive. Our algorithm is applicable to more general systems with finite local complexity and eventually finds all gaps, circumventing an earlier no-go theorem regarding the computability of spectral gaps for general Hamiltonians.

DOI: 10.1103/PhysRevB.106.155140

## I. INTRODUCTION

The spectrum of a periodic Hamiltonian is characterized by bands and gaps or, for example, in the case of incommensurable magnetic fields and two dimensions, by gaps only (Cantor spectrum) [1–4]. Numerical results on finite patches, as well as experimental data, suggest that spectral gaps appear also in systems with aperiodic order, such as the Hofstadter model on a quasicrystal [5–11]. Since Bloch theory is no longer available, alternative methods are needed to compute the spectrum of an infinitely extended aperiodic system. Using the method of quasimodes (also known as "almost eigenvectors"), one can deduce from the spectrum of the Hamiltonian restricted to a finite patch that certain intervals *contain* spectrum of the infinite volume Hamiltonian $H$. See for example [12,13] for efficient implementations of this strategy for aperiodic systems. Nevertheless, crucial physical features of such systems, such as topological phases [14–16], depend on the existence and location of *spectral gaps*, that is the information that certain intervals do *not contain* spectrum of the infinite volume Hamiltonian. However, until now, besides certain specific situations, the location of spectral gaps in aperiodic systems could only be guessed from numerical data on finite patches, but not conclusively confirmed.

In this article, we present a method that allows to actually prove the existence of spectral gaps in infinite aperiodic systems based on numerical calculations on finite domains. Our method can be applied to any kind of short-range Hamiltonian with finite local complexity. We apply it to the Hofstadter Hamiltonian and to the $p_x p_y$ model, both on the Ammann-Beenker tiling. In particular, for the $p_x p_y$ model we prove that a small energy gap is open, which appears in numerical calculations on finite balls, but whose existence for the infinite system was uncertain [11]. This demonstrates that a rigorous procedure like ours can be useful when numerical results are otherwise hard to interpret.

Numerical investigations of aperiodic systems necessarily restrict the Hamiltonian to finite patches and then either apply periodic boundary conditions, or use open boundary conditions. The first method relies on the construction of the so-called periodic approximant systems. While it has been shown that in specific models it is possible to successfully construct such periodic approximants [17,18], the mathematical justification of this procedure for generic aperiodic systems is still subject of ongoing research [19–22]. Furthermore, we stress that usually one does not have a precise control of the rate of convergence of the spectral properties of the periodic approximants. Using open boundary conditions, on the other hand, edge-states may appear in gaps of the *bulk spectrum*, i.e., in the spectrum of the infinite volume Hamiltonian. In previous papers, such edge-states, as shown for example in Fig. 1, have been discarded as "spectral pollution" [12,23]. So far, however, no precise criterion has been formulated to decide whether a given state is an edge state and thus does not contribute to the bulk spectrum. Our result formulated below yields such a criterion. Roughly speaking we show that if for some spectral window all quasimodes appearing in boxes of side-length $2L$ satisfy a quantifiable "edge-state criterion", then this spectral window is a gap in the spectrum of the infinite-volume Hamiltonian. Our criterion can be numerically checked for finite-range Hamiltonians with finite local complexity, where for a given $L > 0$ the restriction of $H$ to a box of side-length $2L$ centered at an *arbitrary* point in space yields a matrix from a *finite* set of possible realizations.

## II. FINITE-SIZE CRITERION FOR SPECTRAL GAPS

### A. General finite-size criterion

We first formulate a general finite-size criterion, which is equivalent to the existence of a bulk gap. This criterion does not depend on the finite local complexity, and we merely assume that the Hamiltonian $H$ is a bounded Hermitian operator on $\ell^2(\Gamma;\mathcal{H})$, where $\mathcal{H}$ is a separable Hilbert space and $\Gamma \subset \mathbb{R}^d$ is a countable set. We will also assume that

 

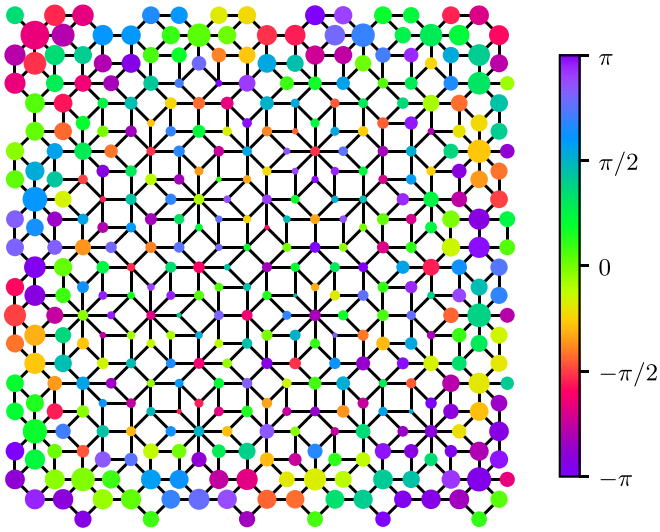


FIG. 1. An edge state of a magnetic Hamiltonian on a finite patch of the Ammann-Beenker tiling ($L = 9$). The color of the dots corresponds to the phase of the wave function and the radius to the modulus. While the infinite system has a spectral gap at this energy, the finite system has an eigenstate whose mass is concentrated at the edges.

there is a maximal distance $r > 0$ such that any point in $\mathbb{R}^d$ is within a distance at most $r$ of a point in $\Gamma$. Throughout this article we measure distances in $\mathbb{R}^d$ using the $\infty$-norm $\|x\|_\infty := \max\{|x_1|, \ldots, |x_d|\}$. We also write

$$B_L(x) := \prod_{j=1}^{d} (x_j - L, x_j + L)$$

for the open cube of side length $2L$ centered around the point $x \in \mathbb{R}^d$ and $\overline{B_L}(x)$ for its closure $\overline{B_L}(x) := \prod_{j=1}^{d} [x_j - L, x_j + L]$. For any set $A \subset \mathbb{R}^d$ and wave function $\psi \in \ell^2(\Gamma; \mathcal{H})$, we denote by

$$\|\psi\|_A^2 := \sum_{x \in \Gamma \cap A} \|\psi(x)\|_{\mathcal{H}}^2$$

its $\ell^2$ mass in $A$.

*Definition 1.* Let $\epsilon, L > 0$ and $\lambda \in \mathbb{R}$. We say that a Hamiltonian $H$ is locally $\epsilon$-bulk gapped at energy $\lambda$ and scale $L$ if there exist constants $N \in \mathbb{N}$, $N \geqslant 2$, and $C < 1/N^d$ such that for any $x \in \Gamma$ and any $\psi \in \ell^2(\Gamma; \mathcal{H})$ we have the following implication: Whenever

$$\|(H - \lambda)\psi\|_{B_L(x)} \leqslant \epsilon \|\psi\|_{B_L(x)}, \tag{1}$$

then for $l := \frac{L+r}{N} + r$ it holds that

$$\|\psi\|_{\overline{B_l}(x)}^2 \leqslant C \|\psi\|_{B_L(x)}^2. \tag{2}$$

In other words, Definition 1 requires that at some scale $L$ all $\epsilon$ quasimodes (1) have an underproportional mass within the bulk (2). Although this property depends only on evaluations of the Hamiltonian $H$ on finite patches, we can show that it implies that the interval $(\lambda - \epsilon, \lambda + \epsilon)$ does not contain any spectrum of $H$.

*Theorem 1.* If a Hamiltonian $H$ on $\ell^2(\Gamma; \mathcal{H})$ is locally $\epsilon$-bulk gapped at energy $\lambda$ on some scale $L > 0$, then the interval $(\lambda - \epsilon, \lambda + \epsilon)$ is a gap in the spectrum of $H$, i.e.,

$$\sigma(H) \cap (\lambda - \epsilon, \lambda + \epsilon) = \varnothing.$$

The complete proof of Theorem 1 is given in Appendix A. However, the underlying geometric idea is easily explained and we sketch it here. Suppose that we are in dimension $d = 1$, and that the statement in Definition 1 holds for $l = L/N$ instead of the more complicated expression involving $r$. We can then show that $H$ has no eigenvalues in $(\lambda - \epsilon, \lambda + \epsilon)$ using a simple decomposition argument: Define the lattices

$$Z_q := 2L(\mathbb{Z} + q/N) \quad \text{for} \quad q \in \{1, \ldots, N\}.$$

While for fixed $q$ the larger open intervals $B_L(x)$ centered at different $x \in Z_q$ are still mutually disjoint, the shorter closed intervals $\overline{B_l}(x)$ cover $\mathbb{R}$ when taking the union over all $q$, i.e.,

$$\bigcup_{q=1}^{n} \bigcup_{x \in Z_q} \overline{B_l}(x) = \mathbb{R}. \tag{3}$$

Now assume that $\psi$ is an eigenfunction of $H$ with eigenvalue $\lambda_0 \in (\lambda - \epsilon, \lambda + \epsilon)$. Then $\psi$ satisfies (1) for any $x$, and thus, by assumption, also (2). This implies

$$\sum_{q=1}^{N} \sum_{x \in Z_q} \|\psi\|_{\overline{B_l}(x)}^2 < \frac{1}{N} \sum_{q=1}^{N} \sum_{x \in Z_q} \|\psi\|_{B_L(x)}^2 = \|\psi\|^2,$$

while (3) implies

$$\sum_{q=1}^{N} \sum_{x \in Z_q} \|\psi\|_{\overline{B_l}(x)}^2 \geqslant \|\psi\|^2.$$

This is a contradiction and thus no such eigenfunction can exist.

### B. A criterion that can be checked numerically

We now discuss how to establish existence of local $\epsilon$-bulk gaps, and thus by Theorem 1 spectral gaps for Hamiltonians with finite-range hoppings and finite local complexity. We first give a sufficient condition for a Hamiltonian to be locally $\epsilon$-bulk gapped that can be easily verified numerically (see Appendix B). From now on we assume that $H$ has only finite-range hoppings with maximal hopping length $m$, namely $H_{xy} = 0$ for all $x, y \in \Gamma$ with $\|x - y\|_\infty > m$. For any set $A \subset \mathbb{R}^d$ we denote by $\mathbf{1}_A$ the characteristic function of $A$ and set $H_A := \mathbf{1}_A H \mathbf{1}_A$.

*Proposition 1.* As before, let $L > 0$, $N \in \mathbb{N}$, $N \geqslant 2$, $l := \frac{L+r}{N} + r$, and $\lambda \in \mathbb{R}$.

Assume that for every $x \in \Gamma$ there exists a set $A(x) \subset \Gamma$ such that $\overline{B_l}(x) \subseteq A(x) \subseteq B_{L-m}(x)$, $\lambda \notin \sigma(H_{A(x)})$, and

$$D(x) = \left\| \mathbf{1}_{\overline{B_l}(x)} (H_{A(x)} - \lambda)^{-1} \mathbf{1}_{A(x)} H \mathbf{1}_{B_L(x) \setminus A(x)} \right\|_{\text{op}}$$

satisfies $D(x) < N^{-d/2}$.

Then $H$ is locally $\epsilon$-bulk gapped at energy $\lambda$ and scale $L$ for any $\epsilon > 0$ with

$$\epsilon < \inf_{x \in \Gamma} \frac{N^{-d/2} - D(x)}{\left\| \mathbf{1}_{\overline{B_l}(x)} (H_{A(x)} - \lambda)^{-1} \mathbf{1}_{A(x)} \right\|_{\text{op}}}. \tag{4}$$

The proof of Proposition 1 is given in Appendix A. Note that $H_{A(x)}$ is a sparse matrix and therefore the conditions of Proposition 1 can be efficiently checked using a sparse LU

factorization [24]. This way, the condition can be verified even for values of $L$ for which a direct diagonalization approach would no longer be computationally feasible.

## III. APPLICATION TO QUASICRYSTALS

In order to apply Proposition 1 to quasicrystals $\Gamma \subset \mathbb{R}^d$, we need a way to enumerate all *local patches*

$$\mathcal{C}_L(x) := \{y \in \mathbb{R}^d \,|\, x + y \in \Gamma \cap B_L(x)\} \subset B_L(0)$$

at scale $L$ that occur for $x \in \Gamma$. We say that $\Gamma$ has *finite local complexity* if the set $\mathcal{C}_L = \{\mathcal{C}_L(x) \,|\, x \in \Gamma\}$ is finite [25–27]. Those quasiperiodic tilings that are suggested as models for physical systems all have finite local complexity. Our method is practical because, for common quasicrystals, the number of local patches grows only polynomially in $L$, while it would grow exponentially without long-range order [28,29].

To enumerate the tilings, we make use of the cut-and-project construction of quasiperiodic tilings [30,31]. The Ammann-Beenker tiling [32,33] can be defined by a cut-and-project method using two "projections",

$$p = \begin{pmatrix} 1 & a & 0 & -a \\ 0 & a & 1 & a \end{pmatrix} \quad \text{and} \quad \kappa = \begin{pmatrix} 1 & -a & 0 & a \\ 0 & a & -1 & a \end{pmatrix},$$

both maps from $\mathbb{R}^4$ to $\mathbb{R}^2$, where $a = 1/\sqrt{2}$. We call $p$ and $\kappa$ "projections" since they represent orthogonal projections onto two orthogonal two-dimensional subspaces of $\mathbb{R}^4$, which are then both identified with $\mathbb{R}^2$. Furthermore, let $R \subset \mathbb{R}^2$ be the regular axis-aligned octagon centered at 0 with side length 1. The vertices of the Ammann-Beenker tiling are the set

$$\Gamma_{\mathrm{AB}} = \{\, p(z) \mid z \in \mathbb{Z}^4,\ \kappa(z) \in R \,\}.$$

An edge is introduced between $p(z_1)$ and $p(z_2)$ whenever $z_1$ and $z_2$ differ by a unit vector in $\mathbb{R}^4$. Because $a$ is irrational, every point $x \in \Gamma_{\mathrm{AB}}$ has exactly one pre-image $z \in \mathbb{Z}^4$ such that $p(z) = x$.

What local patches $\mathcal{C}_L(x)$ can occur when $x$ varies in $\Gamma_{\mathrm{AB}}$? Let $z \in \mathbb{Z}^4$ be such that $p(z) = x \in \Gamma_{\mathrm{AB}}$, and consider the set of all $v \in \mathbb{Z}^4$ such that $p(z + v) \in \Gamma_{\mathrm{AB}} \cap B_L(x)$. There is only a finite number of $v \in \mathbb{Z}^4$ that can occur across all $x$, because $v$ has to fulfill the two conditions,

$$p(z + v) \in B_L(x) \quad \text{and} \quad \kappa(z + v) \in R. \tag{5}$$

By the linearity of $p$, the first condition reduces to

$$p(v) \in B_L(0) \tag{6}$$

and since $\kappa(x) \in R$, the second condition implies

$$\kappa(v) \in 2R, \tag{7}$$

where $2R$ is the octagon of side length 2.

Both (6) and (7) state that a linear image of $v$ lies in some compact set. Since $p$ and $\kappa$ have orthogonal kernels, these two conditions define a set $\tilde{V}_L$ linearly equivalent to the cartesian product of $B_L(0)$ and $2R$, which is itself compact and hence contains only finitely many integer points. Let $V_L = \tilde{V}_L \cap \mathbb{Z}^4$ be this set of "candidate points". An algorithm for computing $V_L$ is described in Appendix B, Algorithm 1.

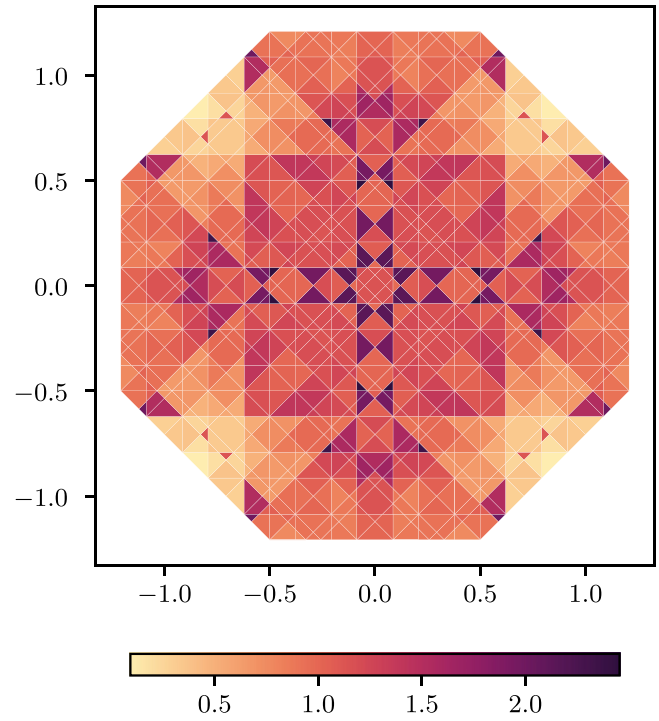


FIG. 2. The octagonal acceptance region for the Ammann-Beenker tiling decomposed into subpolygons corresponding to the different local patches in $\mathcal{C}_L(x)$, for $L = 5$. The color of each polygon corresponds to $D(x)$ computed for $N = 2$ with $A(x) = B_{L-1}(x)$ (in this case $m = 1$), drawn in a logarithmic scale with base 10, for the Hofstadter Hamiltonian at magnetic field $b = 1$ and energy 1.5. At scale $L = 5$, $D(x)$ never falls below the required bound $1/2$. At scale $L = 50$ one finds that $D(x) < 1/2$ for every local patch, proving the gap.

According to (5), for any $v \in V_L$ the patch $\mathcal{C}_L(x)$ contains the point $p(z + v)$ if and only if

$$\kappa(z) \in R - \kappa(v), \tag{8}$$

i.e., if $\kappa(z)$ lies in the shifted octagon $R - \kappa(v)$. Put differently, every candidate point $v \in V_L$ decomposes the octagon $R$ into two disjoint sets $P^0(v)$ and $P^1(v)$, delineating for which $\kappa(z)$ the point $p(z + v)$ is or is not in $\Gamma_{\mathrm{AB}}$. The enumeration algorithm then merely consists of computing all possible intersections $\bigcap_{v \in V} P^{i_v}(v)$, where $i \in \{0, 1\}^{|V|}$. One can show that the number of such intersection that are nonempty, and hence the number of local patches, grows quadratically in $L$ for the Ammann-Beenker tiling [34]. They can be enumerated efficiently using a dynamic programming approach described in Appendix B, Algorithm 2. Figure 2 shows the resulting decomposition of the octagon $R$ for $L = 5$.

### A. Two explicit models

We now study two physical systems on the Ammann-Beenker tiling. The $p_x p_y$ model is a model for a weak topological superconductor whose real-space description allows it to be defined on aperiodic sets [35]. The matrix elements of the Hamiltonian are

$$H_{xy} = -t\sigma_3 - \tfrac{\mathrm{i}}{2}\Delta\sigma_1 \cos(\alpha_{xy}) - \tfrac{\mathrm{i}}{2}\Delta\sigma_2 \sin(\alpha_{xy}),$$
$$H_{xx} = -\mu\sigma_3,$$

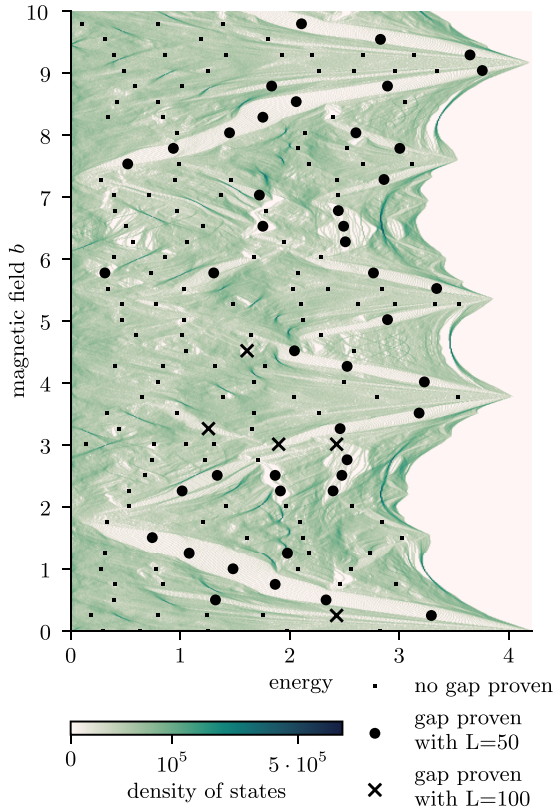


FIG. 3. The Hofstadter butterfly of the magnetic Laplacian on the Ammann-Beenker tiling with some points selected for investigation using our method.

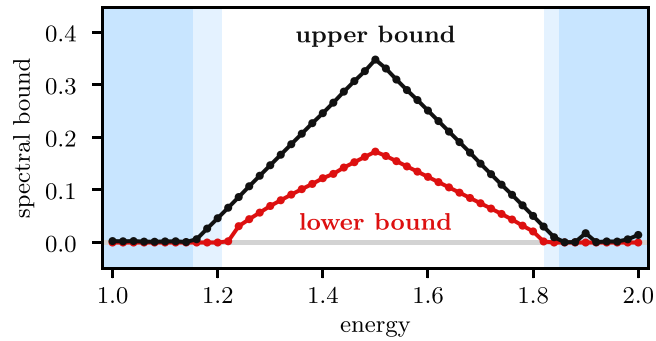


FIG. 4. Comparison of our lower bound for the distance to spectrum (for $L = 50$) to the upper bound computed with the method of [12]. We computed both bounds for 50 equally spaced energies in the Hofstadter model at a constant magnetic field $b = 1$. The combination of these bounds allows us to bound the extent of the spectral gap containing energy 1.5. The endpoints of the gap must be contained in the lighter shaded areas around energies 1.2 and 1.82.

for $\|x - y\|_2 \leqslant 1$, and $H_{xy} = 0$ otherwise. Here $\sigma_1, \sigma_2, \sigma_3$ are Pauli matrices, $\mu, \Delta \in \mathbb{R}$ and $\alpha_{xy}$ is the signed angle between the edge $xy$ and the $e_1$ axis.

For $\mu$ very large, this Hamiltonian can be considered as a small perturbation of $\mu\sigma_3$, thus its spectrum has a gap around 0, without edge states when restricted to finite domains. As $\mu$ decreases, the gap eventually closes and the system is expected to undergo a quantum phase transition into a topologically nontrivial phase. This topological regime has been studied in [11]. Employing computational $K$ theory, convincing evidence was found that a large gap around zero indeed reopens. But the numerical data also suggested a second small gap might open. In the absence of a decisive criterion, the author had to leave open whether this gap persists in the thermodynamic limit [11, p. 9]. Using our method, we could prove that there really is a small second gap around energy 0.804 in the infinite system.

As a second example, we applied our method to the Hofstadter model on the Ammann-Beenker tiling. In the symmetric gauge, the matrix elements of the Hofstadter Hamiltonian are $H_{xy} = \mathrm{e}^{\mathrm{i}b\det(x,y)}$ for $\|x - y\|_2 \leqslant 1$, and $H_{xy} = 0$ otherwise, where $b \in \mathbb{R}$ denotes the strength of the magnetic field perpendicular to the tiling. It was previously observed that patterns related to the Hofstadter butterfly also emerge in quasicrystalline systems [36–38]. We approximated the density of states of the Hofstadter butterfly (see Fig. 3) by diagonalization of a finite system and created a set of possible gap locations by taking all local minima of a kernel density estimate with bandwidth 0.1 of the spectra. In this way we generated 187 combinations of magnetic field and energy where a gap might be expected. Applying our algorithm with $L = 50$, we could show for 44 of these points that there is a spectral gap in the infinite system, increasing to 49 points with $L = 100$. For $L = 50$, this required checking 15 139 local patches, while for $L = 100$, we had $|\mathcal{C}_L| = 60\,601$.

## IV. COMPUTATIONAL COMPLEXITY OF SPECTRAL COMPUTATIONS

We computed a cross section of our lower bound on the distance to the spectrum at different energies for a fixed magnetic field, see Fig. 4. Comparing our lower bound to the upper bound in [12] shows that the curves are similar and increase linearly towards the center of the gap. Both estimates approximate the distance to the spectrum well. See Fig. 5 in the Appendix for a similar plot for the Fibonacci crystal, showing multiple gaps. The combination of both bounds yields rigorous and precise information on the positions of the edge of the spectral gap.

This should be compared to the no-go theorem of [12] that an algorithm with two-sided error control (see Appendix D, Definition 3) for general Hermitian operators on a given Hilbert space does not exist. While the precise formulation of this no-go theorem requires some preparation and is given only in Appendix D, the basic idea is easily explained. An algorithm with two-sided error control has as input a Hamiltonian $H$ from a certain set $\Omega$ of Hamiltonians and an error margin. It is supposed to return a subset of the reals that approximates the spectrum $\sigma(H)$ within the given error margin in Hausdorff distance.

It also needs to be specified which properties of the Hamiltonian the algorithm can access directly. In the setting of the no-go theorem, it can access the matrix elements $H_{ij}$ of $H$ with respect to some orthonormal basis $(e_i)_{i\in\mathbb{N}}$. Of course any algorithm that stops after finite time can evaluate only finitely many matrix elements. Now it is clear that no such algorithm can, for example, after having evaluated a finite number of

matrix elements of an operator in

$$\Omega_{\text{diag}} := \{H = \text{diag}(\lambda_1, \lambda_2, \ldots) \,|\, \lambda_i \in [0,1],\ i \in \mathbb{N}\},$$

decide that any interval $(a, b) \subseteq [0, 1]$ is free of spectrum. To do so, it would have to exclude that $\lambda_i \in (a, b)$ for any $i \in \mathbb{N}$, which is impossible based on a finite sample of the $\lambda_i$. So while one can find convergent approximations to the spectrum, one can never prove the existence of a gap in this example. However, this would be required in order to obtain error control in Hausdorff distance.

Our algorithm circumvents this no-go theorem by assuming the additional structure of finite local complexity and finite-range hoppings (interactions). In fact, one can prove that for any energy $\lambda$ that is not in the spectrum of such a Hamiltonian, it is possible to determine an $L$ with which our algorithm shows that some neighborhood of $\lambda$ is contained in a gap. The required $L$ only depends on the distance to the spectrum as well as on the norm and maximum hopping length of the Hamiltonian. This means that the gap estimate in Fig. 4 can be made arbitrarily accurate by choosing $L$ large enough and computation of the spectrum with two-sided error control is possible in the case of finite local complexity. In the framework of the *solvability complexity index* [39,40], this corresponds to a decrease in the complexity class from $\Sigma_1^A$ to $\Delta_1^A$. More information on this is given in Appendix D.

## V. CONCLUSIONS

We have described a method to systematically and conclusively establish the existence and location of spectral gaps for infinite aperiodic Hamiltonians with finite local complexity. The method is based on the characterization of the support of quasimodes for finite volume subsystems of the aperiodic Hamiltonian: Although a spectral gap may close by introducing boundary conditions on a finite subsystem, the states filling such a bulk gap are localized at the edge of the subsystem. We formulate an edge state criterion, namely Definition 1, and show that if all quasimodes near a certain energy $\lambda$ in all finite patches of a certain size are edge states in the sense of Definition 1, the corresponding energy must be in a bulk gap, see Theorem 1.

We provide a way to check this criterion numerically by computing certain resolvents in the finite systems, that is Proposition 1, which can be implemented efficiently using sparse numerics. We also derive a lower bound for the size of the gap. To apply this method to quasicrystals, we describe an algorithm enumerating all local patches of a quasiperiodic tiling, using the cut-and-project construction of quasicrystals. Based on this, we investigate two physical models on quasicrystals, the $p_x p_y$ model and the Hoftstadter model, and rigorously establish the existence of their spectral gaps, even in situations where previous numerical computations gave inconclusive results [11].

Gaps that are suggested by finite-system computations can be proven to be gaps in the bulk using our method. In fact, one can prove the existence of any gap by choosing the subsystem size large enough. Therefore, we show that, unlike in the general case where only one-sided error control of the spectrum is possible [12], the spectrum of operators with finite local complexity is computable with error control in Hausdorff distance.

Finally, we would like to stress that while in this paper we only apply our method to quasicrystals, the class of operators with finite local complexity is general enough to encompass a wide range of models used in physical applications, such as periodic systems, quasicrystalline materials, systems with edges, heterostructures, or disordered systems. We show that the spectrum is computable with two-sided error control in all such cases (see Appendix D). However, in some systems the number of local patches grows so fast that applying our method may not be practical. For example, in disordered systems, the number of local patches may grow exponentially fast in $L$. Nevertheless, there are many cases of physical interest, for instance low-dimensional defects in quasicrystalline systems or junctions between noncommensurate materials, in which the number of local patches grows only polynomially. In all these cases, our method can easily be adapted to prove the existence of spectral gaps.

## ACKNOWLEDGMENTS

The Authors would like to thank G. Panati for pointing out Ref. [11] and for useful discussions. The work of M.M. is supported by a fellowship of the Alexander von Humboldt Foundation.

## APPENDIX A: FULL MATHEMATICAL PROOFS

In this section we provide a complete proof of Theorem 1 and Proposition 1. For the convenience of the reader, we briefly recall our framework together with relevant definitions and the statements of the results.

The Hamiltonian $H$ is a bounded Hermitian operator on $\ell^2(\Gamma; \mathcal{H})$, where $\Gamma \subset \mathbb{R}^d$ is a countable set and $\mathcal{H}$ is a separable Hilbert space. We assume that there is a maximum distance $r > 0$ such that any point in $\mathbb{R}^d$ is at most a distance $r$ away from a point in $\Gamma$. Recall that distances in $\mathbb{R}^d$ are measured in the norm $\|x\|_\infty := \max\{|x_1|, \ldots, |x_d|\}$. The open cube with side-length $2r$ around $x \in \mathbb{R}^d$ is

$$B_r(x) := \{y \in \mathbb{R}^d \,|\, \|x - y\|_\infty < r\}$$

and its closure $\overline{B_r}(x) := \{y \in \mathbb{R}^d \,|\, \|x - y\|_\infty \leqslant r\}$. For any set $A \subset \mathbb{R}^d$ and wave function $\psi \in \ell^2(\Gamma; \mathcal{H})$, we denote by $\|\psi\|_A^2 := \sum_{x \in \Gamma \cap A} \|\psi(x)\|_{\mathcal{H}}^2$ its $\ell^2$ mass in the region $A$.

Definition 1 makes precise the idea that a Hamiltonian is gapped in the bulk at a certain energy $\lambda$ and a certain length scale $L$, if all $\epsilon$-quasimodes at that energy that are supported in a region of that scale, see (1), are disproportionately supported near the edge of the region (2).

*Definition 1.* Let $\epsilon, L > 0$, and $\lambda \in \mathbb{R}$. We say that a Hamiltonian $H$ is locally $\epsilon$-bulk gapped at energy $\lambda$ and scale $L$ if there exist constants $N \in \mathbb{N}, N \geqslant 2$, and $C < 1/N^d$ such that for any $x \in \Gamma$ and any $\psi \in \ell^2(\Gamma; \mathcal{H})$ we have the following implication: Whenever

$$\|(H - \lambda)\psi\|_{B_L(x)} \leqslant \epsilon \|\psi\|_{B_L(x)}, \tag{1}$$

then for $l := \frac{L+r}{N} + r$ it holds that

$$\|\psi\|_{\overline{B_l}(x)}^2 \leqslant C \|\psi\|_{B_L(x)}^2. \tag{2}$$

In the following we call any $\psi \in L^2(\mathbb{R}^d)$ that satisfies the inequality (1) an $L$-local $\epsilon$-quasimode at $x$. In these terms, Definition 1 says that every $L$-local $\epsilon$-quasimode at $x$ has most of its mass in $B_L(x)$ concentrated outside of $\overline{B_l}(x)$. This terminology is useful in the proof of the main theorem.

*Theorem 1.* If a Hamiltonian $H$ on $\ell^2(\Gamma;\mathcal{H})$ is locally $\epsilon$-bulk gapped at energy $\lambda$ on some scale $L > 0$, then the interval $(\lambda-\epsilon, \lambda+\epsilon)$ is a gap in the spectrum of $H$, i.e.,

$$\sigma(H) \cap (\lambda-\epsilon, \lambda+\epsilon) = \varnothing.$$

*Proof.* Assume that $H$ is locally $\epsilon$-bulk-gapped at energy $\lambda$ and scale $L > 0$. Let $l, N$ and $C$ be as in Definition 1. We generalise the proof strategy presented in the main text. For every $q \in \{1,\dots,N\}^d$ let

$$\widetilde{Z}_q := 2(L+r)(\mathbb{Z}^d + q/N) \tag{A1}$$

and

$$f_q : \widetilde{Z}_q \to \Gamma,\ \widetilde{x} \mapsto f_q(\widetilde{x}) := \text{the point in } \Gamma \text{ closest to } \tilde{x}. \tag{A2}$$

In the case where several points in $\Gamma$ minimize the distance to $\widetilde{x}$, we arbitrarily pick one of them in the definition of $f_q(\widetilde{x})$. By the assumption on $\Gamma$ we have that $\|\widetilde{x} - f_q(\widetilde{x})\|_\infty \leqslant r$ for all $\widetilde{x} \in \widetilde{Z}_q$. Since two distinct points in $\widetilde{Z}_q$ have at least distance $2(L+r)$, this implies that the map $f_q$ is one-to-one. Hence, as a map onto its image

$$Z_q := f_q(\widetilde{Z}_q) \subset \Gamma, \tag{A3}$$

the map $f_q : \widetilde{Z}_q \to Z_q$ is a bijection and we think of $Z_q$ as a deformation of $\widetilde{Z}_q$.

It is now straightforward to see that the large boxes $B_L(x)$ are still mutually disjoint when $x$ varies in one of the deformed sublattices $Z_q$ and that the small boxes $\overline{B_l}(x)$ still cover all of $\mathbb{R}^d$ if $x$ varies in the union $\cup_q Z_q$:

*Disjointness:* For any $q \in \{1,\dots,N\}^d$ and two different points $x, y \in Z_q$

$$B_L(x) \cap B_L(y) = \varnothing. \tag{A4}$$

*Proof.* Let $\widetilde{x} := f_q^{-1}(x)$ and $\widetilde{y} := f_q^{-1}(y)$. Then $\widetilde{x}$ and $\widetilde{y}$ are two distinct points in the square lattice $\widetilde{Z}_q$ and thus their distance is at least $2(L+r)$. Using the inverse triangle inequality we conclude that

$$\begin{aligned}\|x-y\|_\infty &= \|\tilde{x}-\tilde{y}+x-\tilde{x}+\tilde{y}-y\|_\infty \\ &\geqslant \|\tilde{x}-\tilde{y}\|_\infty - \|x-\tilde{x}\|_\infty - \|\tilde{y}-y\|_\infty \\ &\geqslant 2(L+r) - 2r \\ &= 2L.\end{aligned}$$

Thus, the boxes $B_L(x)$ and $B_L(y)$ do not overlap. ∎

*Covering:*

$$\bigcup_{q\in\{1,\dots,N\}^d} \bigcup_{x\in Z_q} \overline{B_l}(x) = \mathbb{R}^d. \tag{A5}$$

*Proof.* Note that the union

$$\widetilde{Z} := \bigcup_{q\in\{1,\dots,N\}^d} \widetilde{Z}_q$$

is a square lattice with side length $2(L+r)/N$. Thus, for every $p \in \mathbb{R}^d$, there exists a $q \in \{1,\dots,N\}^d$ and $\widetilde{x} \in \widetilde{Z}_q$ such that $\|p - \widetilde{x}\|_\infty \leqslant (L+r)/N$. The triangle inequality now implies

$$\begin{aligned}\|p - f_q(\widetilde{x})\|_\infty &\leqslant \|p-\widetilde{x}\|_\infty + \|\widetilde{x} - f_q(\widetilde{x})\|_\infty \\ &\leqslant (L+r)/N + r = l\end{aligned} \tag{A6}$$

and therefore $p \in \overline{B_l}(x)$ for $x := f_q(\widetilde{x}) \in Z_q$. ∎

These two properties allow us to prove by contradiction that the spectrum $\sigma(H)$ does not contain the interval $(\lambda-\epsilon, \lambda+\epsilon)$.

Suppose there exists $\nu \in (\lambda-\epsilon, \lambda+\epsilon) \cap \sigma(H)$. Then, according to Weyl's criterion, there exist arbitrarily precise quasimodes for the energy $\nu$. More precisely, for any $\delta > 0$ there exists $\psi \in \ell^2(\Gamma, \mathcal{H})$ such that

$$\|\psi\| = 1 \quad \text{and} \quad \|(H-\nu)\psi\| < \delta. \tag{A7}$$

We now fix $\delta > 0$ such that

$$\delta < (\epsilon - |\lambda - \nu|)^2, \tag{A8a}$$

$$\delta < N^{-d} - C, \tag{A8b}$$

and choose a corresponding $\psi \in \ell^2(\Gamma, \mathcal{H})$ that satisfies (A7).

Notice that if $\psi$ is a $\delta$-quasimode on $\mathbb{R}^d$, this does not imply that $\psi$ is an $L$-local $\delta$-quasimode for all $x \in \mathbb{R}^d$. However, we have that the total mass of $\psi$ on those squares $B_L(x)$ for which $\psi$ is not an $L$-local $\delta$-quasimode is small (it is of order $\delta$). To see this, we split each $Z_q$ into two subsets

$$Z_q^+ := \left\{x \in Z_q \mid \|(H-\nu)\psi\|_{B_L(x)} \leqslant \sqrt{\delta}\|\psi\|_{B_L(x)}\right\},$$

$$Z_q^- := \left\{x \in Z_q \mid \|(H-\nu)\psi\|_{B_L(x)} > \sqrt{\delta}\|\psi\|_{B_L(x)}\right\}.$$

Around the points $x \in Z_q^+$, $\psi$ is an $L$-local $\epsilon$-quasimode, since

$$\begin{aligned}\|(H-\lambda)\psi\|_{B_L(x)} &\leqslant \|(H-\nu)\psi\|_{B_L(x)} + |\lambda-\nu|\|\psi\|_{B_L(x)} \\ &\leqslant (\sqrt{\delta} + |\lambda-\nu|)\|\psi\|_{B_L(x)} \\ &< \epsilon\|\psi\|_{B_L(x)}.\end{aligned} \tag{A9}$$

For the last step of the above, we rewrite (A8a) as

$$\begin{aligned}\delta < (\epsilon - |\lambda-\nu|)^2 &\Rightarrow \sqrt{\delta} < \epsilon - |\lambda-\nu| \\ &\Rightarrow \sqrt{\delta} + |\lambda-\nu| < \epsilon.\end{aligned}$$

Since $H$ is locally $\epsilon$-bulk-gapped on the scale $L$, (A9) implies that for every $x \in Z_q^+$ the inequality (2) holds true. Summing over all $x \in Z_q^+$, we get

$$\sum_{x\in Z_q^+} \|\psi\|^2_{\overline{B_l}(x)} \leqslant C \sum_{x\in Z_q^+} \|\psi\|^2_{B_L(x)}. \tag{A10}$$

By the disjointness condition shown before, we have that $B_L(x)$ and $B_L(y)$ are disjoint for different $x$ and $y$ in $Z_q^+$. Since for disjoint sets $A$ and $B$, we have $\|\psi\|_A^2 + \|\psi\|_B^2 = \|\psi\|^2_{A\cup B}$, we obtain

$$\sum_{x\in Z_q^+} \|\psi\|^2_{B_L(x)} = \|\psi\|_U^2 \leqslant \|\psi\|^2 = 1 \tag{A11}$$

for $U := \bigcup_{x\in Z_q^+} B_L(x)$. Combining Eqs. (A11) and (A10), we get

$$\sum_{x\in Z_q^+} \|\psi\|^2_{\overline{B_l}(x)} \leqslant C. \tag{A12}$$

Let now $x \in Z_q^-$, then by definition of $Z_q^-$ we have

$$\|\psi\|^2_{B_L(x)} < \frac{1}{\delta}\|(H-\nu)\psi\|^2_{B_L(x)}. \tag{A13}$$

By taking the sum over all $x \in Z_q^-$ we get

$$\begin{aligned}\sum_{x\in Z_q^-}\|\psi\|^2_{\overline{B_l}(x)} &\leqslant \sum_{x\in Z_q^-}\|\psi\|^2_{B_L(x)} < \frac{1}{\delta}\sum_{x\in Z_q^-}\|(H-\nu)\psi\|^2_{B_L(x)}\\ &\leqslant \frac{1}{\delta}\|(H-\nu)\psi\|^2,\end{aligned}$$

where we used the disjointness of the $B_L(z)$ for $z \in Z_q$ in the last step. Since $\psi$ is a $\delta$-quasimode, meaning $\|(H-\nu)\psi\|^2 < \delta^2$, we get

$$\sum_{x\in Z_q^-}\|\psi\|^2_{\overline{B_l}(x)} < \delta. \tag{A14}$$

Combining (A12) and (A14) and using the covering property (A5), we finally obtain

$$\begin{aligned}\|\psi\|^2 &\leqslant \sum_{q\in\{1,\dots,N\}^d}\sum_{x\in Z_q}\|\psi\|^2_{\overline{B_l}(x)}\\ &= \sum_{q\in\{1,\dots,N\}^d}\left(\sum_{x\in Z_q^+}\|\psi\|^2_{\overline{B_l}(x)} + \sum_{x\in Z_q^-}\|\psi\|^2_{\overline{B_l}(x)}\right)\\ &\leqslant \sum_{q\in\{1,\dots,N\}^d}(C+\delta) = N^d(C+\delta) \;<\; 1,\end{aligned}$$

where in the last inequality we used the hypothesis (A8b) on $\delta$. Since $\|\psi\|^2 < 1$ contradicts the normalisation of $\psi$ assumed in (A7), such a $\delta$-quasimode cannot exist, and $\nu$ is not in the spectrum of $H$. ∎

*Remark 1.* Notice that neither Definition 1 nor Theorem 1 require the boundedness of the Hamiltonian and can be easily generalized to unbounded operators taking into account only vectors that belong to the domain of the Hamiltonian.

Next we prove the numerically verifiable criterion for the property of being locally $\epsilon$-bulk gapped. Recall that for any set $A \subset \mathbb{R}^d$ we denote by $\mathbf{1}_A$ the characteristic function of $A$ and we use the shorthand notation $H_A := \mathbf{1}_A H \mathbf{1}_A$.

*Proposition 1.* As before, let $L > 0$, $N \in \mathbb{N}$, $N \geqslant 2$, $l := \frac{L+r}{N} + r$, and $\lambda \in \mathbb{R}$.

Assume that for every $x \in \Gamma$ there exists a set $A(x) \subset \Gamma$ such that $\overline{B_l}(x) \subseteq A(x) \subseteq B_{L-m}(x)$, $\lambda \notin \sigma(H_{A(x)})$, and

$$D(x) = \left\|\mathbf{1}_{\overline{B_l}(x)}(H_{A(x)}-\lambda)^{-1}\mathbf{1}_{A(x)}H\mathbf{1}_{B_L(x)\setminus A(x)}\right\|_{\mathrm{op}}$$

satisfies $D(x) < N^{-d/2}$.

Then $H$ is locally $\epsilon$-bulk gapped at energy $\lambda$ and scale $L$ for any $\epsilon > 0$ with

$$\epsilon < \inf_{x\in\Gamma}\frac{N^{-d/2}-D(x)}{\left\|\mathbf{1}_{\overline{B_l}(x)}(H_{A(x)}-\lambda)^{-1}\mathbf{1}_{A(x)}\right\|_{\mathrm{op}}}. \tag{4}$$

*Proof.* Let $x \in \Gamma$ and suppose that for some $\psi \in \ell^2(\Gamma;\mathcal{H})$ property (1) holds, i.e.,

$$u := \mathbf{1}_{B_L(x)}(H-\lambda)\psi$$

satisfies

$$\|u\| < \epsilon\|\psi\|_{B_L(x)}, \tag{A15}$$

with $\epsilon > 0$ satisfying (4). We need to show that this implies (2). Writing

$$\begin{aligned}&(H_{A(x)}-\lambda)\mathbf{1}_{A(x)}\psi\\ &\quad= \mathbf{1}_{A(x)}(H-\lambda)\mathbf{1}_{A(x)}\psi\\ &\quad= \mathbf{1}_{A(x)}(H-\lambda)\psi - \mathbf{1}_{A(x)}(H-\lambda)\mathbf{1}_{A(x)^c}\psi\\ &\quad= \mathbf{1}_{A(x)}u - \mathbf{1}_{A(x)}H\mathbf{1}_{A(x)^c}\psi\end{aligned}$$

and multiplying this equality by $(H_{A(x)}-\lambda)^{-1}$ gives

$$\mathbf{1}_{A(x)}\psi = (H_{A(x)}-\lambda)^{-1}(\mathbf{1}_{A(x)}u + \mathbf{1}_{A(x)}H\mathbf{1}_{A(x)^c}\psi).$$

Since we need to estimate $\|\psi\|_{\overline{B_l}(x)}$, we can multiply by $\mathbf{1}_{B_l(x)}$ to obtain

$$\mathbf{1}_{B_l(x)}\psi = \mathbf{1}_{\overline{B_l}(x)}(H_{A(x)}-\lambda)^{-1}(\mathbf{1}_{A(x)}u + \mathbf{1}_{A(x)}H\mathbf{1}_{A(x)^c}\psi).$$

Using the triangle inequality, we obtain

$$\|\psi\|_{\overline{B_l}(x)} \leqslant Q_1 + Q_2 \tag{A16}$$

with

$$\begin{aligned}Q_1 &= \left\|\mathbf{1}_{\overline{B_l}(x)}(H_{A(x)}-\lambda)^{-1}\mathbf{1}_{A(x)}u\right\|\\ Q_2 &= \left\|\mathbf{1}_{\overline{B_l}(x)}(H_{A(x)}-\lambda)^{-1}\mathbf{1}_{A(x)}H\mathbf{1}_{A(x)^c}\psi\right\|.\end{aligned}$$

The first term is easily bounded using (A15),

$$Q_1 < M(x)\,\epsilon\|\psi\|_{B_L(x)}$$

with

$$M(x) := \left\|\mathbf{1}_{\overline{B_l}(x)}(H_{A(x)}-\lambda)^{-1}\mathbf{1}_{A(x)}\right\|_{\mathrm{op}}.$$

Because of the finite-range hypothesis on $H$ and the fact that $A(x) \subset B_{L-m}(x)$, we can rewrite the second term $Q_2$ using

$$\begin{aligned}&\mathbf{1}_{\overline{B_l}(x)}(H_{A(x)}-\lambda)^{-1}\mathbf{1}_{A(x)}H\mathbf{1}_{A(x)^c}\psi\\ &\quad= \mathbf{1}_{\overline{B_l}(x)}(H_{A(x)}-\lambda)^{-1}\mathbf{1}_{A(x)}H\mathbf{1}_{B_L(x)\setminus A(x)}\psi.\end{aligned}$$

Thus, $Q_2$ can be estimated using the assumption on $D(x)$ and we find that

$$\begin{aligned}\|\psi\|_{\overline{B_l}(x)} &< M(x)\,\epsilon\|\psi\|_{B_L(x)} + D(x)\|\psi\|_{B_L(x)\setminus A(x)}\\ &\leqslant (D(x)+\epsilon M(x))\|\psi\|_{B_L(x)}.\end{aligned}$$

Since (4) implies that

$$\begin{aligned}\sup_{x\in\Gamma}(D(x)+\epsilon M(x))^2 &< \sup_{x\in\Gamma}\left(D(x)+\frac{N^{-d/2}-D(x)}{M(x)}M(x)\right)^2\\ &= N^{-d},\end{aligned}$$

(2) holds for any $C$ with

$$\sup_{x\in\Gamma}(D(x)+\epsilon M(x))^2 < C < N^{-d}.$$

∎

## APPENDIX B: DESCRIPTION OF THE ALGORITHMS

In this section we explain in detail how to apply the general results of Theorem 1 to Hamiltonians modelled over the Ammann-Beenker tiling by enumerating all local patches on a certain scale $L$ and then checking the conditions of

Proposition 1. The method can be easily generalised to other cut-and-project tilings. Moreover, Proposition 1 can be applied in principle to any Hamiltonian that has finite local complexity. The problem of enumerating all possible local restrictions of $H_{B_L(x)}$ on a scale $L$ then needs to be solved in a way specific to the structure of $\Gamma$ and $H$.

We first describe an algorithm to determine all the different local patches that can occur in the Ammann-Beenker quasicrystal $\Gamma_{\mathrm{AB}}$ defined with the cut-and-project method, that is to determine the set $\mathcal{C}_L := \{\mathcal{C}_L(x) \,|\, x \in \Gamma_{\mathrm{AB}}\}$ of all local patches $\mathcal{C}_L(x) := \{y \in \mathbb{R}^d \,|\, x + y \in \Gamma_{\mathrm{AB}} \cap B_L(x)\}$.

Recall that the vertices of the Ammann-Beenker tiling are defined as the set

$$\Gamma_{\mathrm{AB}} = \{\, p(z) \mid z \in \mathbb{Z}^4,\ \kappa(z) \in R \,\},$$

where $a = \frac{1}{\sqrt{2}}$, $R \subset \mathbb{R}^2$ is the regular axis-aligned octagon centered at 0 with side length 1, and

$$p = \begin{pmatrix} 1 & a & 0 & -a \\ 0 & a & 1 & a \end{pmatrix}, \quad \kappa = \begin{pmatrix} 1 & -a & 0 & a \\ 0 & a & -1 & a \end{pmatrix}$$

are the two "projections" as maps from $\mathbb{R}^4$ to $\mathbb{R}^2$.

The first algorithm we describe determines the set $V_L \subseteq \mathbb{Z}^4$ of "candidate points" defined as

$$V_L = \{\, v \in \mathbb{Z}^4 \mid p(v) \in B_L(0) \text{ and } \kappa(v) \in 2R \,\}.$$

As explained in the main text, this set is defined such that for every $z \in \mathbb{Z}^4$, the points of $\Gamma_{\mathrm{AB}} \cap B_L(p(z))$ are all of the form $p(z + v)$ for some $v \in V_L$. Thus to determine which points are part of the local patch around $p(z)$, we only need to check the points $z + v$ for $v \in V_L$.

The set of candidate points $V_L$ only depends on $L$ and hence we only have to compute it once at the beginning of the algorithm. To compute it, it would be possible in principle to simply check the two conditions $p(v) \in B_L(0)$ and $\kappa(v) \in 2R$ for all integer points in a four-dimensional cube around 0 with radius $2L$, say, but this would be very inefficient as it requires checking $O(L^4)$ points. Because the condition $\kappa(v) \in R$ means that all points in $V_L$ lie close to the two-dimensional hyperplane defined by $\kappa(v) = 0$, it should only be necessary to check the conditions for $O(L^2)$ points.

To compute $V_L$ efficiently, consider the matrix

$$t = \begin{pmatrix} 1 & 0 \\ a & a \\ 0 & 1 \\ -a & a \end{pmatrix}.$$

The matrix $t$ satisfies $\kappa t = 0$ and $pt = 2 \cdot \mathbf{1}$. Because the columns of $t$ together with the second and fourth canonical basis vectors $e_2$ and $e_4$ form a linear basis of $\mathbb{R}^4$, we can write any $v \in V_L$ as

$$v = t\begin{pmatrix} w_1 \\ w_2 \end{pmatrix} + q_1 e_2 + q_2 e_4 = \begin{pmatrix} w_1 \\ a(w_1 + w_2) + q_1 \\ w_2 \\ a(w_2 - w_1) + q_2 \end{pmatrix}. \quad \text{(B1)}$$

Because $v \in \mathbb{Z}^4$, also $w_1, w_2 \in \mathbb{Z}$. The condition $\kappa v \in 2R$ that holds for all $v \in V_L$ can be used to bound $q_1$ and $q_2$. In fact, using $\kappa t = 0$ we conclude that

$$\begin{pmatrix} a & a \\ -a & a \end{pmatrix}\begin{pmatrix} q_1 \\ q_2 \end{pmatrix} = \kappa(q_1 e_2 + q_2 e_4) = \kappa(v) \in 2R. \quad \text{(B2)}$$

Since the matrix

$$A = \begin{pmatrix} a & a \\ -a & a \end{pmatrix},$$

and hence also its inverse, are symmetries of $R$ (that is, $AR = R$), (B2) just becomes

$$\begin{pmatrix} q_1 \\ q_2 \end{pmatrix} \in 2R.$$

In particular, this condition on $(q_1, q_2)$ is independent of $L$. This is what allows enumerating all points according to Eq. (B1) with $q_1, q_2$ in only $O(L^2)$ steps.

We now compute the range of values that $w_1$ and $w_2$ can take such that (B1) defines an element $v \in V_L$. Using

$$pt = \begin{pmatrix} 2 & 0 \\ 0 & 2 \end{pmatrix},$$

we find

$$p(v) = p\left[t\begin{pmatrix} w_1 \\ w_2 \end{pmatrix} + q_1 e_2 + q_2 e_4\right] = 2\begin{pmatrix} w_1 \\ w_2 \end{pmatrix} + A^T\begin{pmatrix} q_1 \\ q_2 \end{pmatrix}.$$

As also $A^T$ leaves $R$ invariant, $(q_1, q_2) \in 2R$ implies

$$p(v) - 2\begin{pmatrix} w_1 \\ w_2 \end{pmatrix} \in 2R.$$

Since $v \in V_L$ requires $pv \in B_L(0)$ and since the $\infty$-norm of $2R$ is bounded by $1 + \sqrt{2}$, we find that

$$2\begin{pmatrix} w_1 \\ w_2 \end{pmatrix} \in B_{L+1+\sqrt{2}}(0).$$

Thus $w_1$ and $w_2$ must both lie in the interval $(-L/2 - s, L/2 + s)$ with $s = (1 + \sqrt{2})/2$.

Thus, when determining whether $v \in \mathbb{Z}^4$ lies in $V_L$, the values of $v_1 = w_1$ and $v_3 = w_2$ can be restricted to integers in this range (line 1 in Algorithm 1). For $q_1$ and $q_2$, it suffices to consider all values in $2R \subset B_{2s}(0)$ such that the resulting values for $v_2$ and $v_4$ become integral (line 2 in Algorithm 1).

Next, we describe the algorithm to enumerate the local patches of the Ammann-Beenker tiling. As we have discussed in the main text, the local patch $\mathcal{C}_L(x)$ centered at $x = p(z) \in \Gamma_{\mathrm{AB}}$ can be characterized by which of the candidate points in $V_L$ "become part of the tiling". Namely, for every $v \in V_L$, we

Algorithm 1. Enumerate "candidate set" $V_L$.

1: **for all** integers $v_1, v_3$ in $(-L/2 - s, L/2 + s)$ **do**
2: **for all** integers $v_2 \in a(v_1 + v_3) + [-2s, 2s]$ and $v_4 \in a(v_1 - v_3) + [-2s, 2s]$ **do**
3: **if** $p(v) \in B_L(0)$ and $\kappa(v) \in 2R$ **then**
4: add $v$ to $V_L$
5: **end if**
6: **end for**
7: **end for**

have

$$p(z+v) \in \Gamma_{\mathrm{AB}} \Leftrightarrow \kappa(z+v) \in R \Leftrightarrow \kappa(z) \in R - \kappa(v). \quad \text{(B3)}$$

Defining for $v \in \mathbb{R}^4$ the following decomposition of the acceptance region,

$$P^1(v) := R \cap (R - \kappa(v))$$
$$P^0(v) := R \setminus P^1(v),$$

(B3) entails that for every $v \in V_L$ it holds that

$$p(v) \in \mathcal{C}_L(x) \Leftrightarrow \kappa(z) \in P^1(v). \quad \text{(B4)}$$

By labeling the points in the set $V_L$ with an index $i \in \{1, \ldots, |V_L|\}$, we can uniquely associate to each bit string $b = (b_1, \ldots, b_{|V_L|}) \in \{0,1\}^{|V_L|}$ a local patch

$$\mathcal{C}_{L,b} := \{\, p(v_i) \,|\, b_i = 1, i \in \{1, \ldots, |V_L|\}\}.$$

From (B4) we conclude that

$$\mathcal{C}_L(x) = \mathcal{C}_{L,b} \Leftrightarrow \kappa(z) \in P_{(b_i)} := \bigcap_{i=1}^{|V_L|} P^{b_i}(v_i). \quad \text{(B5)}$$

For many bit strings $b$ the set $P_{(b_i)}$ turns out to be empty and thus not all local patches $\mathcal{C}_{L,b}$ defined by bit strings $b$ of length $|V_L|$ correspond to actual local patches of the Ammann-Beenker tiling. In fact, the number of local patches (also referred to as the "patch counting function" or, in [34], "complexity") of the Ammann-Beenker tiling is of order $O(L^2)$, cf. [34], while the number of possible bit strings is $O(2^{|V_L|})$, with $|V_L|$ growing like $L^2$.

To enumerate those bit strings that correspond to actual local patches (i.e., for which the set $P_{(b_i)}$ is not empty), we can use a dynamic programming approach. To do so, we first extend the definition (B5) of $P_{(b_i)}$ to shorter bit strings $(b_i)$, namely to $(b_i) \in \{0,1\}^m$, $1 \leqslant m \leqslant |V_L|$, by taking into account only the intersections up to the $m$th place of the bit string.

Our algorithm then proceeds step by step by computing all nonempty $P_{(b_i)}$ for bit strings $(b_i)$ of length 1, of length 2, and so on. By (B5), we can go from a bit string of length $n$ to a bit string of lenght $n+1$ using the following recursion relation:

$$P_{(b_i)\oplus 1} = P_{(b_i)} \cap P^1(v_{i+1}),$$
$$P_{(b_i)\oplus 0} = P_{(b_i)} \cap P^0(v_{i+1}). \quad \text{(B6)}$$

Suppose we have computed a set $J_n$ of all bit strings $(b_i)$ of length $n$ and their associated sets $P_{(b_i)}$ for all $(b_i)$ where $P_{(b_i)}$ is not empty. We can then compute the set $J_{n+1}$ by computing, for every $(b_i) \in J_n$, the two intersections on the right hand sides of (B6) and adding those of the two bit string $(b_i) \oplus 0$ and $(b_i) \oplus 1$ for which the intersection is not zero. This procedure can be implemented algorithmically by simply maintaining a list $J$ of nonempty regions $P_{(b_i)}$ and the associated bit strings, as described in the pseudocode in the loop in line 2 of Algorithm 2. The following algorithm is formulated to decompose an area $R_0 \subseteq R$. While setting $R_0 = R$ will lead to an enumeration of all patches, it is sometimes advantageous to compute only the decompositions corresponding to $\kappa(z) \in R_0$ for some smaller $R_0$, as described in Algorithm 2.

Usually we decompose the entire region of acceptance $R$ according to the previous procedure. However, it can be useful to decompose only a smaller polygon $R_0 \subseteq R$. The reason for this is twofold. First, there are some symmetries of $R$, which can allow us to decompose a smaller region. For example, the tiling corresponding to $\kappa(z) = (k_1, k_2)$ is exactly the mirror image of the tiling corresponding to $(k_2, k_1)$. Therefore, considering

$$R_0 := R \cap \{(x,y) \in \mathbb{R}^2 \,|\, x > 0, y > 0, y < x\},$$

is sufficient for enumerating all local patches up to all mirror symmetries. In that case one may replace $R$ by $R_0$ in Algorithm 2.

Apart from the case where one has to check only part of the acceptance region $R$ for symmetry reasons, splitting $R$ into subpolygons can improve the performance of the algorithm. In the default case, for every candidate point $v_i \in V_L$, the intersection of the set $P^1(v_i)$ with all polygons $P_{(b_j)}$ distinguished up to that point has to be computed. The time taken for this appears to be quadratic in the final number $|\mathcal{C}_L|$ of local patches distinguished. If one only computes the decomposition of a smaller polygon $R' \subseteq R$, the intersection computation can be skipped in all cases where either $R' \subseteq P^1(v_i)$ or $R' \subseteq P^0(v_i)$, because the intersections are trivial (either empty or all of $P_{(b_j)}$). This is implemented in lines 2 to 13 of Algorithm 2 by replacing $R$ by $R'$. In practice, we have found that splitting the region $R$ into many convex polygonal pieces $R'_j$, such that $\bigcup_j R'_j = R_0$ (we used 80 pieces $R'_j$ for $L = 100$) greatly improved the running time of the algorithm. The fact that some tilings could occur in several of the pieces was found to play a negligible role in terms of performance. Additionally, this method allows the algorithm to be parallelized across multiple cores or nodes, since the computation for every piece $R'_i$ is independent of all others.

Algorithm 2. Enumerate the local patches $\mathcal{C}_L(x)$.

1: Initialize $J = \{(R_0, \text{`}\,\text{'})\}$.
2: Compute $V_L$ using Algorithm 1
3: **for all** $v \in V_L$ **do**
4: set $P^1(v) = R - \kappa(v)$.
5: Initialize $J_2 = \{\}$
6: **if** $R_0 \subseteq P^1(v)$
7: set $J \leftarrow \{(Q, s \oplus \text{`1'}) \,|\, (Q,s) \in J\}$
8: **continue** with next $v$
9: **end if**
10: **if** $R_0 \cap P^1(v) = \varnothing$ **then**
11: set $J \leftarrow \{(Q, s \oplus \text{`0'}) \,|\, (Q,s) \in J\}$
12: **continue** with next $v$
13: **end if**
14: **for all** $(Q,s) \in J$ **do**
15: **if** $P^1(v) \cap Q \neq \varnothing$ **then**
16: Add $(P \cap Q, s \oplus \text{`1'})$ to $J_2$
17: **end if**
18: **if** $Q \backslash P^1(v) \neq \varnothing$ **then**
19: Add $(Q \backslash P, s \oplus \text{`0'})$ to $J_2$
20: **end if**
21: **end for**
22: Update $J \leftarrow J_2$.
23: **end for**

Having enumerated the candidate set, we now describe how to use the enumeration Algorithm 2 to check whether the Hamiltonian on each patch satisfies the condition in Proposition 1. Specifically, we have to compute the norms

$$D(x) = \left\| \mathbf{1}_{\overline{B_l}(x)} (H_{A(x)} - \lambda)^{-1} \mathbf{1}_{A(x)} H \mathbf{1}_{B_L(x)\setminus A(x)} \right\| \tag{B7}$$

and check that

$$D(x) < N^{-d/2} \tag{B8}$$

for all $x \in \Gamma$. Let us first explain in detail how we choose $A(x)$. Since the norm of $(H_{A(x)} - \lambda)^{-1}$ is expected to fall off exponentially in the distance between $\mathbf{1}_{\overline{B_l}(x)}$ and $\mathbf{1}_{A(x)} H \mathbf{1}_{B_L(x)\setminus A(x)}$, $D(x)$ is expected to be minimal for $A(x) = B_{L-m}(x)$. It turns out that this is true in most cases. However, if $\lambda$ is very close to the spectrum of $H_{B_{L-m}(x)}$, which happened in our simulations only for a few local patches, then the norm of $(H_{B_{L-m}(x)} - \lambda)^{-1}$ and thus $D(x)$ may become too large. In those cases we computed (B7) again with a different choice of $A(x)$. We found that already removing one site chosen at random from the edge set $\Gamma_{\mathrm{AB}} \cap (B_{L-m}(x) \setminus B_{L-m-1}(x))$ from $B_{L-m}(x)$ was usually enough to perturb the spectrum of $H_{B_{L-m}(x)}$ sufficiently to remove outliers in the value of $D(x)$.

To actually compute the norm in (B7), the most obvious method would be to invert $(H_{A(x)} - \lambda)$, compute the matrix products as written, and then compute the norm. However, computing matrix inverses is expensive and prone to numerical error, and it would not be feasible at all for matrices of the size we are considering in this paper. The method of computing $D(x)$ we present now, by contrast, even works with sparse matrices, which makes it efficient enough that it can be employed for values of $L$ where an investigation of the spectrum of $H_{B_L(x)}$ by direct diagonalization would not be possible. (Although many algorithms are of course available for approximating the spectrum of sparse Hermitian operators [41].)

Instead of computing the matrix product as written in the right-hand side of (B7), we compute the individual entries of the matrix. Let $M(x) := \mathbf{1}_{\overline{B_l}(x)} (H_{A(x)} - \lambda)^{-1} \mathbf{1}_{A(x)} H \mathbf{1}_{B_L(x)\setminus A(x)}$. Then, for $\tilde{x} \in \Gamma \cap \overline{B_l}(x)$ and $\tilde{y} \in \Gamma \cap (B_L(x) \setminus A(x))$, we compute the matrix entries

$$M(x)_{\tilde{x}\tilde{y}} = \mathbf{1}_{\{\tilde{x}\}} (H_{A(x)} - \lambda)^{-1} \mathbf{1}_{A(x)} H \mathbf{1}_{\{\tilde{y}\}}.$$

Depending on whether there are more $\tilde{x}$'s or $\tilde{y}$'s to consider, we compute either the vector

$$\mathbf{1}_{\{\tilde{x}\}} (H_{A(x)} - \lambda)^{-1} \mathbf{1}_{A(x)} H$$

or

$$(H_{A(x)} - \lambda)^{-1} \mathbf{1}_{A(x)} H \mathbf{1}_{\tilde{y}}.$$

This is easier because for a given vector $\mathbf{z}$ we can compute $(H_{A(x)} - \lambda)\mathbf{z}$ using the sparse matrix $H_{A(x)}$. The efficiency of the algorithm can be greatly increased by preparing a decomposition of $(H_{A(x)} - \lambda)$ that can be used to solve $(H_{A(x)} - \lambda)^{-1}\mathbf{z}$ for different vectors $\mathbf{z}$; we use a sparse LU decomposition [24] for our computations. We then compute the norm $D(x)$ from these matrix entries. Algorithm 3 describes the computation we use to check (B8).

The two branches of the "if" statement in line 3 of Algorithm 3 always compute the same number, and the condition is only an optimization that transposes the matrix product in (B7) in order to reduce the number of linear systems that have to be solved.

Finally, Algorithm 4 summarizes our general strategy, using the enumeration of the local patches from Algorithm 2 and

Algorithm 3. Check Eq. (B8).

1: Compute the sparse LU factorization of $H_{A(x)} - \lambda$
2: Initialize an empty matrix $m \times n$ matrix $T$, where
   $m = |B_l(x)|_\Gamma$ and $n = |B_L(x)\setminus A(x)|_\Gamma$
3: **if** $n < m$ **then**
4:  **for all** $\tilde{y} \in (B_L(x)\setminus A) \cap \Gamma$ **do**
5:  Set $b = (H\delta_{\tilde{y}})|_{A(x)}$ as a vector in $l^2(A(x) \cap \Gamma)$
6:  Solve $(H_{A(x)} - \lambda)y = b$ using the LU factorization
7:  Put $y$ in the column of $T$ corresponding to $\tilde{y}$
8:  **end for**
9: **else**
10:  Initialize an $m \times P$ matrix $\tilde{T}$, where $P = |A(x)|_\Gamma$.
11:  **for all** $\tilde{x} \in B_l(x) \cap \Gamma$ **do**
12:  Set $b = \delta_{\tilde{x}}$ as a vector in $l^2(A \cap \Gamma)$
13:  Solve $(H_{A(x)} - \lambda)y = b$ using the LU factorization
14:  Put $y$ in the row of $\tilde{T}$ corresponding to $\tilde{x}$
15:  **end for**
16:  Set $T = \tilde{T} H \mathbf{1}_{B_L(x)\setminus A(x)}$, an $m \times n$ matrix.
17:  Set $D(x) = \|T\|_{\mathrm{op}}$ and check $D(x) < N^{-d/2}$.
18: **end if**

Algorithm 4. Prove a gap at energy $\lambda$.

1: Split the region $R$ into $n$ smaller polygons
   $R_1, \ldots, R_j, \ldots, R_n$ (for efficiency)
2: **for all** polygons $R_j$ **do**
3:  Using Algorithm 2, decompose $R_j$ into a number of
   polygons $P_{(b_i)}$ corresponding to local patches in $\mathcal{C}_L$.
4:  Initialize $r_{\min,j} = \infty$, the minimum gap size
5:  **for all** polygons $P_{(b_i)}$ corresponding to a bit string $(b_i)$ **do**
6:  Construct the Hamiltonian $H$ on $B_L(x)$, for an $x$
   with $\kappa(p^{-1}(x)) \in P_{(b_i)}$
7:  Generate a finite list $A_k$ of values of $A(x)$ to try.
   We always set $A_1 = B_{L-m}(x)$, while $A_2, A_3, \ldots, A_t$ are
   generated by removing random points from the edge of $A_1$.
8:  **for all** $A = A_1, A_2, \ldots, A_t$ **do**
9:  Set $A = B_{L-m}(x)$
10:  Use Algorithm 3 to check Eq. (B8)
11:  **if** Eq. (B8) is fulfilled **then**
12:  Set $r_{\min,j} \leftarrow \min(r_{\min,j}, \epsilon]$, where $\epsilon$ is the
   maximum allowed by Eq. (4).
13:  **continue** with next polygon $P_{(b_i)}$
14:  **end if**
15:  **end for**
16:  **if** Eq. (B8) was not fulfilled for any $A$ **then**
17:  **end computation**, no gap could be proven
18:  **end if**
19:  **end for**
20:  Let $r_{\min} = \min(r_{\min,1}, \ldots, r_{\min,n})$
21:  **end computation**, the infinite Hamiltonian has a gap
   of size $r_{\min}$ at energy $\lambda$.
22: **end for**

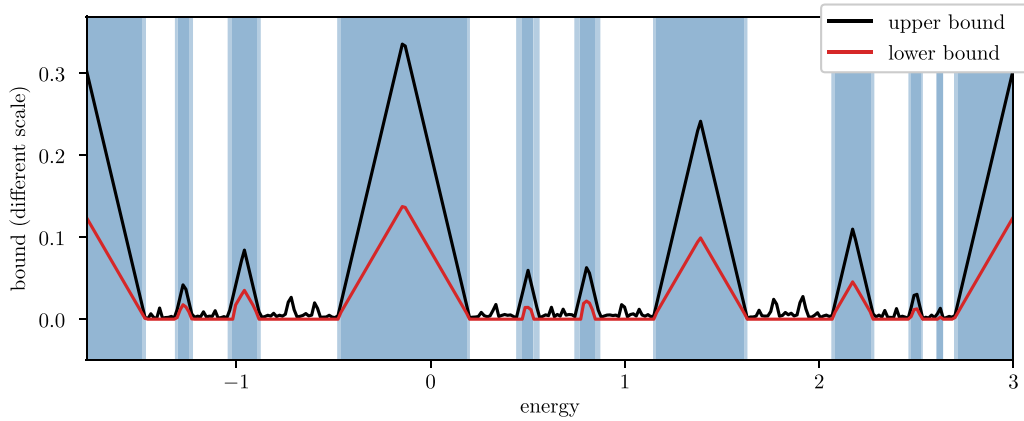


FIG. 5. Upper and lower bounds for the distance to the spectrum for the Fibonacci Hamiltonian for $L = 500, N = 6, \alpha = 1$. The transparent blue intervals display the minimal and maximal sizes (defined as in Fig. 4) of the gaps centered around the local maxima of the lower bound. For the Fibonacci quasicrystal, multiple gaps can be seen and proven to exist. As $L \to \infty$, the number of gaps will grow as the spectrum of the infinite Hamiltonian is a Cantor set.

checking the condition of Propositon 1 on each of them using Algorithm 3. The loop in line 4 can be performed on different computer nodes if necessary.

## APPENDIX C: APPLICATION TO ONE-DIMENSIONAL SYSTEMS

The Fibonacci quasicrystal is a simple one-dimensional quasicrystal that was studied even prior to the discovery of physical quasicrystals [42,43]. In recent years, significant attention has been devoted to the mathematical rigorous study of the spectrum of the Hamiltonian associated to the Fibonacci quasicrystals [44–46] and also of its generalization for continuum Schrödinger operators [47,48]. In particular, it has been proved that the spectrum of the Fibonacci Hamiltonian is a Cantor set [49,50]. In this section, we will describe how our method can be applied to systems in one dimension using the explicit example of the Fibonacci quasicrystal, which has the advantage that many of the constructions are easier to visualize in such case. In particular, we compute upper and lower bound for the distance to the spectrum for the Fibonacci Hamiltonian, which clearly show the fractal structure of its spectrum, see Fig. 5.

### 1. Cut-and-project construction of the Fibonacci quasicrystal

As in the Ammann-Beenker case, we will define two projections, in this case from $\mathbb{R}^2$ to $\mathbb{R}$, corresponding respectively to the real space and to the additional dimension,

$$p = (1 \quad \varphi) \quad \kappa = (-\varphi \quad 1), \tag{C1}$$

where $\varphi := \frac{1+\sqrt{5}}{2}$ is the golden ration. Clearly the kernels of $p$ and $\kappa$ are again orthogonal.

The acceptance region in the case of the Fibonacci quasicrystal consists simply of the interval

$$R = [0, 1). \tag{C2}$$

This is the projection of the vertical interval $\{0\} \times [0, 1)$ via $\kappa$.

We can then define the Fibonacci lattice as

$$\Gamma_{\text{Fib}} = \{\, p(z) \mid z \in \mathbb{Z}^2,\ \kappa(z) \in R \,\}.$$

The condition $\kappa(z) \in R$ corresponds to the "cutting" step, the expression $p(z)$ is the "projection" step.

Figure 6 contains a pictorial representation of this cut-and-project construction. The yellow shaded area in Fig. 6 shows points in $\mathbb{R}^2$ for which $\kappa(z) \in R$.

This definition of the Fibonacci quasicrystal is equivalent to the more common one that uses the substitution rules

$$\mathrm{S} \to \mathrm{L} \quad \mathrm{L} \to \mathrm{LS}.$$

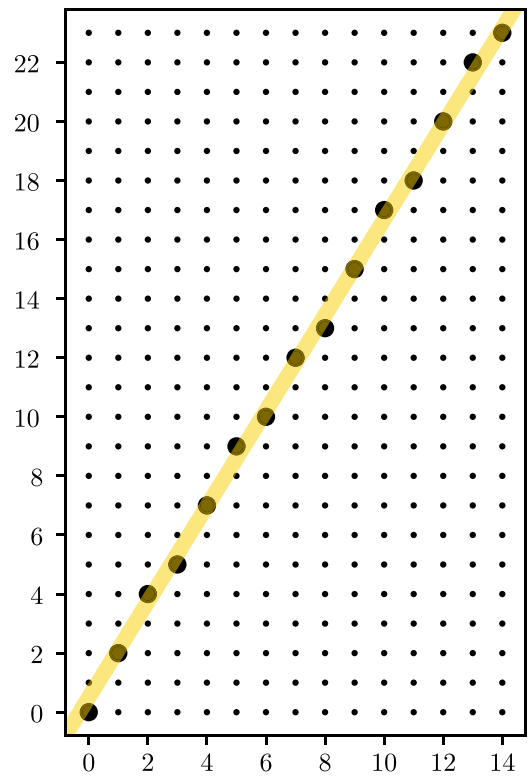


FIG. 6. Cut-and-project construction of the Fibonacci quasicrystal.

Starting from the string "L", this substitution rule gives a sequence of strings "LS", "LSL", "LSLLS", "LSLLSLSL"... in which the $n$th string is a prefix of the $(n+1)$-th and a suffix of the $(n+2)$th. This allows one to define a Fibonacci string that is infinite in both directions.

The equivalence is based on the fact that neighboring points in the Fibonacci lattice form either "long" or "short" distances, corresponding to the letters "L" and "S" in the substitution definition. As one can see in Fig. 6, successive points $z$ with $\kappa(z) \in R$ always differ by either the vector (1, 1) or the vector (1,2). Under the projection $p$, these vectors map to offsets

$$(1+\varphi) \quad \text{and} \quad (1+2\varphi).$$

The intervals of length $(1+2\varphi)$ are the "long" intervals L and the intervals of length $(1+\varphi)$ are the "short" intervals S. The quotient between the lengths is again $\varphi$.

### 2. Enumeration of local patches

Let us show how to enumerate all local patches $\mathcal{C}_L$ of the Fibonacci quasicrystal. As in the case of the Ammann-Beenker tiling, for any $x \in \Gamma_{\text{Fib}}$, the *local patch around* $x$ is the set

$$\mathcal{C}_L(x) = \{\, \tilde{x} - x \,|\, \tilde{x} \in \Gamma_{\text{Fib}} \cap B_L(x) \,\}.$$

Since every point in $x \in \Gamma_{\text{Fib}}$ has exactly one preimage $z \in \mathbb{Z}^2$ with $p(z) = x$ and $\kappa(z) \in R$, by exploiting the linearity of $p$ and $\kappa$, the set of local patch can be rewritten in the usual form as

$$\mathcal{C}_L(x) = \{\, p(v) \mid v \in \mathbb{Z}^2, \kappa(v) \in R - \kappa(z), |p(v)| < L\}.$$

This description of the local patch only depends on $\kappa(z)$, where $z$ is the integer preimage of $x$ under $p$ (which is unique by irrationality considerations). Our enumeration algorithm will decompose the interval [0,1) in which $\kappa(z)$ lies into subintervals corresponding to different local patches.

It turns out that for any given $L$, there are only finitely many points $v \in \mathbb{Z}^2$, which can fulfill the two conditions $\kappa(v) \in R - \kappa(z)$ and $|p(v)| < L$, across all $z \in \mathbb{Z}^2$ with $\kappa(z) \in R$. Indeed, for a point $v \in \mathbb{Z}^2$ to be able to satisfy the condition $\kappa(v) \in R - \kappa(z)$ for any $z$ with $\kappa(z) \in R$, we must have

$$\kappa(v) \in R + (-R)$$

where $R + (-R)$ denotes the Minkowski sum. This equals the interval $R + (-R) = (-1, 1)$. As for the Ammann-Beenker tiling, we define the set of "candidate points" as

$$V_L := \{v \in \mathbb{Z}^2 \,|\, \kappa(v) \in (-1, 1)\,;\, p(v) \in (-L, L)\,\}.$$

Because the two projections $p$ and $\kappa$ have orthogonal kernels, the two sets where the two conditions $\kappa(v) \in (-1, 1)$ and $p(v) \in (-L, L)$ respectively are fulfilled are two orthogonal strips, whose intersection is a rectangle, as shown in Fig. 7. Any finite rectangle contains a finite number of points, therefore the set $V_L$ is finite.

It is also easy to enumerate these candidate points algorithmically. To do so we describe here an algorithm similar to Algorithm 1 that we used for the Ammann-Beenker tiling. In this case we can choose any vector in $\mathbb{R}^2$ to be a right inverse for $p$ (up to a constant factor) and we just need to impose that such vector is in the kernel of $\kappa$. Consider the vector $t := (1 \;\; \varphi)$, we have $pt = (1+\varphi^2)$ and we also have that $\kappa t = 0$. Therefore, every point $v \in V_L$ can be written as

$$v = ty + qe_2$$

for some $y, q \in \mathbb{R}$. Moreover, $v \in \mathbb{Z}^2$ implies that $y \in \mathbb{Z}$, while $\kappa v \in (-1, 1)$ implies that $q \in (-1, 1)$. Thus, any candidate point is of the form $v = (v_1, v_2)$, with $v_1 \in \mathbb{Z}$ and $v_2 \in \varphi v_1 + (-1, 1)$. If we then consider also the condition $pv \in (-L, L)$, we get that $v_1 \in \frac{(-L,L)+(-1,1)}{1+\varphi^2}$. In particular, if we want to count all the candidate points $v$ such that $pv \in I$, with $I$ a given interval, we have to enumerate all the integers $v_1, v_2$ such that

$$v_1 \in \frac{I + (-1, 1)}{1+\varphi^2} \qquad v_2 \in \varphi v_1 + (-1, 1),$$

which results in two loops (over $v_1$ and $v_2$) similar two the loops in Algorithm 1.

As we have explained in Appendix B, once a set of candidate points has been computed, we can categorize the values $\kappa(z)$ by which local patch we get. The local patch is completely determined by which points $z + v \in \mathbb{Z}^2$ become part of the tiling. All points in the candidate set $V_L$ fulfill

$$|p(v)| < L.$$

Therefore $|p(z+v) - p(z)| < L$. Thus, the condition $|p(\tilde{z}) - p(z)| < L$ is always fulfilled for all points in our candidate set.

Instead, whether the other condition is fulfilled, namely $\kappa(\tilde{z}) \in R$, depends on the base point $z$, or more precisely on $\kappa(z)$. We have $\kappa(\tilde{z}) = \kappa(z+v) = \kappa(z) + \kappa(v) \in R$, which implies

$$\kappa(z) \in R - \kappa(v). \tag{C3}$$

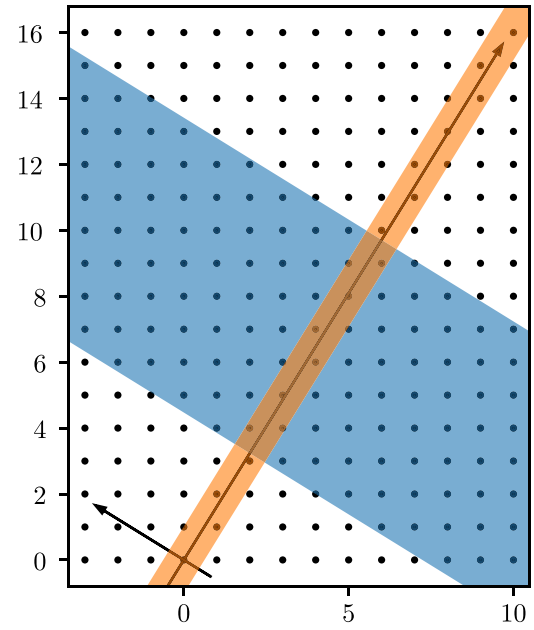


FIG. 7. The set of candidate points is defined by the two constraints $|p(v)| < L$ and $\kappa(v) \in (-1, 1)$. In this picture, the constraint on $p(v)$ is indicated by the blue shaded area, and the restriction on $\kappa(v)$ by the orange shaded area. Because the projections have orthogonal kernel, it is clear that the intersection of both sets is compact and contains only finitely many integer points.

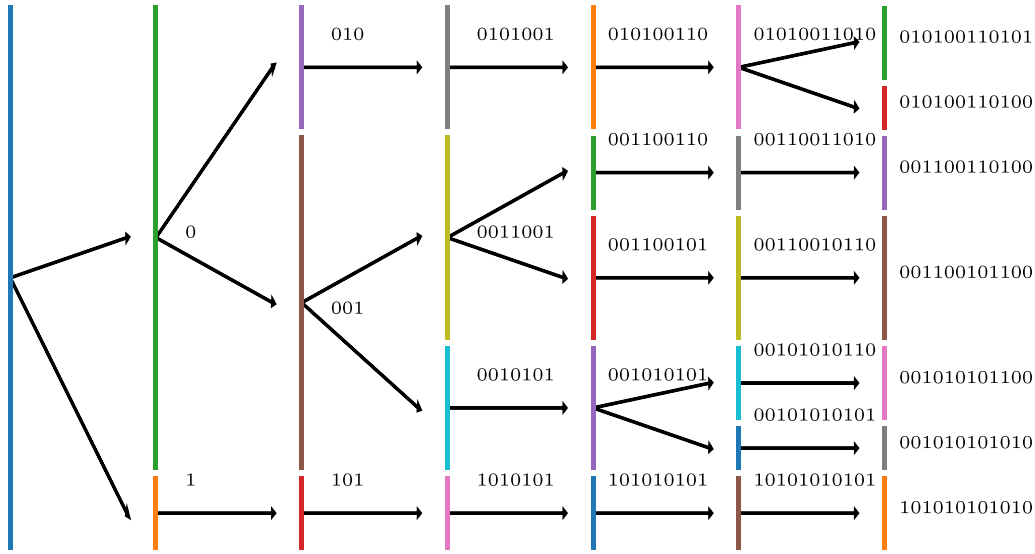


FIG. 8. Successive splitting of the intervals as more candidate points are added, for $L = 10$. The intervals correspond to the sets $P_{(b_i)}$, the strings to the partial bit strings $b$. The large blue interval on the left-hand side is the interval [0,1) associated to the empty string. Steps where no interval is split are not shown.

For a given candidate point $v \in V_L$, the right hand side of (C3) is just an interval, thus for every candidate point $v \in V_L$, we get one such interval. The local patch of scale $L$ around $p(z)$ only depends on which of these intervals the point $\kappa(z)$ lies in.

Let us enumerate the candidate points as $V_L = \{v_i \,|\, i = 1, \ldots, |V_L|\}$. This corresponds to an enumeration of the corresponding intervals $I_i = R - \kappa(v_i)$. Now, a local patch can be described by a bit string $b \in \{0, 1\}^{|V_L|}$, by setting $b_i = 1$ if $\kappa(z) \in I_i$ and $b_i = 0$ otherwise.

Of course, not every bit string will occur in this way. For every bit string $b$, the portion of the acceptance region for which this patch occurs is given by

$$P_{(b_i)} = \bigcap_{i=1}^{|V_L|} P^{b_i}(v_i)$$

where

$$P^1(v_i) = R \cap I_i, \quad P^0(v_i) = R \setminus P^1(v_i).$$

For every $k = \kappa(z) \in P_{(b_i)}$, the bit string associated to the local patch around $x = p(z)$ is exactly $P_{(b_i)}$. If a bit string $b = (b_i)$ does not actually occur, the set $P_{(b_i)}$ will be empty.

To enumerate all actually possible bit strings $(b_i)$, we can start with only the first candidate point $\{v_1\}$, then with the first two $\{v_1, v_2\}$ and so on, proceeding iteratively. As in Appendix B, we extend the notation $P_{(b_i)}$ to bit strings of length $|b| \leqslant |V_L|$ simply by setting

$$P_{(b_i)} = \bigcap_{i=1}^{|b|} P^{b_i}(v_i).$$

For every candidate we add, we can go from a bit string of length $n$ to a bit string of length $n + 1$ using the following recursion relation:

$$P_{(b_i)\oplus 1} = P_{(b_i)} \cap P^1(v_{i+1}), \quad P_{(b_i)\oplus 0} = P_{(b_i)} \cap P^0(v_{i+1}).$$

This suggests a simple algorithm for the enumeration of all nonempty $P_{(b_i)}$, with string length $|b| = |V_L|$, and their associated bit strings.

The algorithm consists of $|V_L| + 1$ steps, $k = 0, \ldots, |V_L|$. At every step, we maintain a list $L_k$ of all bit strings $b$ of length $k$ for which $P_{(b_i)}$ is nonempty, together with the associated $P_{(b_i)}$. Initially, the list only consists of the empty bit string $\varnothing$. The associated set is $S_\varnothing = [0, 1)$.

In the $k$th step, we are given the list $L_{k-1}$ and want to compute $L_k$. So for every bit string $b \in L_{k-1}$, we compute the two sets $S_{b0}$ and $S_{b1}$ as described above, which simply amounts to an intersection of intervals. In many cases, one of these sets will be empty (but not both). We then add to the list $L_k$ all those strings $b' = (b'_i)$ for which $P_{(b'_i)}$ is not empty. In the end, the list $L_{|V_L|}$ will contain all the bit strings $b$ for which $P_{(b_i)} \neq \varnothing$. See Fig. 8 for a visualization of this interval splitting procedure.

### 3. Gap bounds

With the method of enumerating local patches of the tiling described above, we will now describe how our lower bound and the upper bound of [12] can be computed in the Fibonacci case.

We consider the Fibonacci Hamiltonian given by the standard Laplacian on $\ell^2(\mathbb{Z})$ with an electric potential given by the Fibonacci sequence. That is, if we denote by $f(n)$ the sequence with $f(n) = 1$ if the $n$th character of the infinite Fibonacci sequence is $L$ and $f(n) = 0$ otherwise, we can define an operator on $\ell^2(\mathbb{Z})$ by

$$H_{xy} = \begin{cases} \alpha f(x) & x = y \\ -1 & |x - y| = 1\,, \\ 0 & \text{otherwise} \end{cases}$$

where $\alpha \in \mathbb{R}$ is a constant. For $\alpha = 0$, the operator is the standard Laplacian on $\ell^2(\mathbb{Z})$ with absolutely continuous spectrum. As $\alpha$ moves away from 0, gaps will open in the spectrum

of the Laplacian. An enumeration of the local patch of the Fibonacci string can be made similarly to what is described above.

The upper bound of [12] becomes quite simple in a one-dimensional setting like ours. Indeed, following the procedure described in [12], in order to compute the upper bound to the distance to the spectrum of a given energy $\lambda$, one is reduced to analyze the rectangular matrix

$$B = \mathbf{1}_{[-(n+1),\ldots,n+1]}(H - \lambda\mathbf{1})\mathbf{1}_{[-n,n]}.$$

Let $s$ be the lowest eigenvalue of $B^*B$, then the upper bound on the distance from $\lambda$ to the spectrum that is given in [12] is simply $\sqrt{s}$. Although we could verify that the algorithm utilizing the Cholesky decomposition to compute $s$ given in [12] is faster for large sparse matrices, a standard eigenvalue decomposition was sufficient to compute the values corresponding to the black line in Fig. 5.

To compute our lower bound, an enumeration of the possible tilings as outlined above was first made. Using $N = 6$ and $r = 1$, we split each interval $B_L(x)$ into an outer part $B_L(x)\backslash A(x)$, a middle part $A(x)\backslash B_l(x)$ and an inner part $B_l(x)$. It turned out that it was sufficient to always pick the maximal choice $A(x) = B_{L-1}(x)$. This way, the outer part $B_L(x)\backslash A(x)$ has only two elements. Thus, to compute the norm in (4), we only need to compute

$$\mathbf{1}_{\overline{B_l(x)}}(H_{A(x)} - \lambda)^{-1}\mathbf{1}_{A(x)}H\mathbf{1}_{B_L(x)\backslash A(x)}\tilde{\mathbf{x}}_i$$
$$= \mathbf{1}_{\overline{B_l(x)}}(H_{A(x)} - \lambda)^{-1}\mathbf{1}_{A(x)}H\tilde{\mathbf{x}}_i$$

for the two vectors $\tilde{\mathbf{x}}_1 = \delta_{x+L}$ and $\tilde{\mathbf{x}}_2 = \delta_{-L+x}$. The constant $M^{-1}(x)$ may be computed as the lowest eigenvalue of the matrix

$$\mathbf{1}_{\overline{B_{l(x)}}}(H - \lambda)\mathbf{1}_{B_{L-1}(x)}.$$

The values of this lower bound are plotted as the red curve in Fig. 5. It can be seen that our method can resolve even the fine fractal gap structure of the Fibonacci Hamiltonian and gives exact bounds on the extent of gaps of different orders of magnitude.

## APPENDIX D: FURTHER DETAILS ON THE COMPUTATIONAL COMPLEXITY OF SPECTRAL COMPUTATIONS

The existence of the algorithm presented in this paper seemingly contradicts the statement in [12] that it is impossible to compute spectra with error control in a general setting. In fact, even the spectrum of a diagonal operator on an infinite Hilbert space cannot be computed by an algorithm accessing the matrix elements one-by-one. It is only by requiring the additional structure of finite local complexity that such an algorithm can be found. This can be further elucidated in the framework of the *solvability complexity index* (SCI) [39,40,51]: We show that computing the spectrum of an operator of finite local complexity and finite-range hoppings is a problem that can be solved with error control, whereas it is known that this is not possible in the general case [39].

*Definition 2.* A *computational problem* consists of a tuple $(\Omega, \Lambda, (\mathcal{M}, d), \Xi)$. Here $\Omega$ is the domain, or the set of problems. (In our case, $\Omega$ will be a set of operators on a Hilbert space.) The metric space $(\mathcal{M}, d)$ is the set of possible solutions, which in our case will be the power set of $\mathbb{R}$ equipped with the Hausdorff metric, i.e., the possible spectra of Hermitian operators. The *problem function* $\Xi : \Omega \to \mathcal{M}$ describes the exact solution of the problem (for example, the function that maps every operator to its spectrum). Finally, $\Lambda$ is a set of functions, $f_i : \Omega \to \mathbb{R}$, the *evaluation functions*, which the algorithm uses to access information on the given object in $\Omega$.

The role of the evaluation function is to provide information about the objects in $\Omega$ in a form that can be used by the numerical algorithm. In the original formulation of [39], the evaluation functions will just evaluate matrix entries $\langle e_i|H|e_j\rangle$ in some given basis $(e_i)_{i\in\mathbb{N}}$ of the Hilbert space. The set of evaluation function plays a critical role in the formulation of a problem. If we restrict the set of operators $\Omega$ to operators possessing a particular structure (such as finite local complexity below), we will have to change the set of evaluation functions to allow the algorithm to make use of this additional structure. For example, when discussing the spectral problem for periodic operators, the evaluation functions would have to make information about the periods accessible to the algorithm.

*Definition 3.* A computational problem $(\Omega, \Lambda, (\mathcal{M}, d), \Xi)$ is said to have solvability complexity index 1 if and only if there exists a sequence $\Gamma_n$ of functions $\Gamma_n : \Omega \to \mathcal{M}$ such that:

(1) Every function $\Gamma_n$ can be computed using a finite number of elementary arithmetical operations and comparisons from a finite number of evaluations $f_i : \Omega \to \mathbb{R}$.

(2) For every $A \in \Omega$, the computations $\Gamma_n(\Omega)$ converge to $\Xi$ that is

$$d(\Gamma_n(A), \Xi(A)) \to 0 \quad \text{as } n \to \infty.$$

We write $\Delta_2^A$ for the set of all problems with solvability complexity index 1.

If in addition we have that for every $A \in \Omega$, the computations $\Gamma_n(\Omega)$ converge to $\Xi$ in a controlled way, that is

$$d(\Gamma_n(A), \Xi(A)) < 2^{-n}, \tag{D1}$$

we say that the computational problem $(\Omega, \Lambda, (\mathcal{M}, d), \Xi)$ is *solvable with two-sided error control*. The set of all computational problem that is solvable with error control is denoted by $\Delta_1^A$.

The condition (D1) is equivalent to giving an algorithm $\Gamma_n$ and a computable (without limits) error control function $E_n : \Omega \to \mathbb{R}$ such that $d(\Gamma_n(A), \Xi(A)) < E_n(A)$ for all $A \in \Omega$ and $E_n(A) \to 0$ as $n \to \infty$. This can be proven by passing to a subsequence [40].

We can also define the class $\Delta_0^A$ as the set of all computational problems for which there is a single algorithm $\Gamma$ that requires only a finite number of elementary arithmetical operations and evaluations and such that $\Gamma(A) = \Xi(A)$ for all $A \in \Omega$. This class is said to have solvability complexity index equal to zero.

It is also possible to further characterize the problems with solvability complexity 1 that are not solvable with two-sided error control. One can consider the intermediate classes $\Sigma_1^A$ and $\Pi_1^A$, which are defined to provide error control in only one direction (this requires the set of solutions $\mathcal{M}$ to be a ordered by set inclusion, as in the case of the spectral problem). For

example, we say that a problem is in class $\Sigma_1^A$ if $\Gamma_n(A) \to \Xi(A)$ and there exist $X_n(A) \in \mathcal{M}$ such that $\Gamma_n(A) \subseteq X_n(A)$, and $d(X_n(A), \Xi(A)) < 2^{-n}$.

These classes define a hierarchy of sets of computational problems arranged as follows:

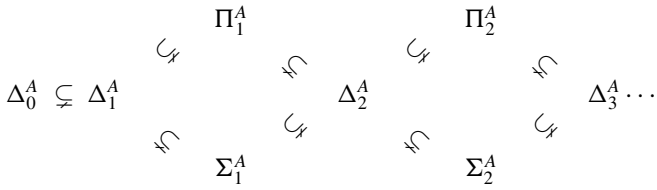


We will not use the higher complexity classes $\Pi_2^A$, $\Sigma_2^A$, $\Delta_3^A$. They describe computational problems for which several limits are needed, for example a family (or "tower") $\Gamma_{m,n}$ of algorithms such that

$$\lim_{m\to\infty} \lim_{n\to\infty} \Gamma_{m,n}(A) = \Xi(A)$$

for all $A \in \Omega$. Such classes are needed for more complex spectral problems, concerning nonself-adjoint operators for example. See [39,40] for precise definitions and applications. The superscript $A$ in the complexity classes defined above refers to the *arithmetic towers of algorithms* [40]. One can define analogous hierarchies of classes by allowing different operations in the algorithms $\Gamma_n$, for example taking radicals or arbitrary functions.

The general spectral problem, even for finite-range self-adjoint operators on a Hilbert space, is not solvable with two-sided error control [39]; In fact, we have the following no-go theorem:

*Theorem 2.* For every $N_{\max} \in \mathbb{R}$ and $m \in \mathbb{R}$, define the set $\Omega$ as the set of all Hamiltonians $H$ on uniformly discrete sets $\Gamma$ with $\|H\|_{\text{op}} \leqslant N_{\max}$ and maximum hopping length $m$, together with an enumeration $(e_i)_{i\in\mathbb{N}}$ of $\Gamma$. Let $\Lambda$ be the set of functions

$$f_{ij}(A) = \langle \delta_{e_i} | A | \delta_{e_j} \rangle$$

evaluating the matrix entries of an operator. Then the computational problem $(\Omega, \Lambda, (\mathcal{M}, d), \Xi|_\Omega)$ is not in $\Delta_1^A$.

The proof of this no-go theorem is surprisingly simple and works independently of the operations allowed for the algorithms in the tower. In fact, the authors remark that it even generalizes to the class of *diagonal operators*. It is based on the fact that any algorithm can only see a finite part of a given infinite matrix, and by changing the matrix in one place outside this range, we can change the spectrum in a way that cannot be detected by the given algorithm (the counterexample matrix thus depends on the algorithm).

While the general spectral problem is thus not in $\Delta_1^A$, one can still determine algorithmically sets that are provably close to parts of the spectrum. But one can never be sure to have found all parts of the spectrum. Put differently, one can not detect gaps and the general spectral problem is therefore in $\Sigma_1^A$, with only one-sided error control possible [12].

It was suggested in [40, Remark 9.1] that it might be a fruitful avenue of research to find some additional structure under which one can reduce the SCI, and that this could lead to new algorithms. We show here, using the algorithm described in the previous sections, that by adding the structure of *finite local complexity*, two-sided error control becomes possible, and the spectral problem in this setting is therefore in $\Delta_1^A$.

*Definition 4.* A *Hamiltonian on a set* $\Gamma$ is a bounded self-adjoint operator on the Hilbert space $\ell^2(\Gamma, \mathcal{H})$, for some finite-dimensional Hilbert space $\mathcal{H}$.

*Definition 5.* A set $\Gamma \subseteq \mathbb{R}^d$ is called *uniformly discrete* if there exists an $\epsilon > 0$ such that every two points $x, y \in \Gamma$ have distance $d(x, y) \geqslant \epsilon$.

*Definition 6.* A set $\Gamma \subseteq \mathbb{R}^d$ is said to have *finite local complexity* if for every $L$, the set

$$\mathcal{C}_L = \{\{y - x | y \in \Gamma, d(x, y) < L\} \,|\, x \in \Gamma\},$$

called the set of *local patches*, is finite.

*Definition 7.* Let $\Gamma$ be a uniformly discrete set. A Hamiltonian $H$ on $\ell^2(\Gamma, \mathcal{H})$ is said to have equivalent action on $B_L(x)$ and $B_L(y)$ if

$$(B_L(x) \cap \Gamma) - x = (B_L(y) \cap \Gamma) - y,$$

and if there are unitaries $U(z) \in \mathcal{U}(\mathcal{H})$ for every $z \in B_L(x) - x$ (defining the change of gauge in the case of the magnetic Hamiltonian) such that for every $t_1, t_2 \in (B_L(x) \cap \Gamma) - x$ we have

$$H_{x+t_1,x+t_2} = U(t_1)^* H_{y+t_1,y+t_2} U(t_2).$$

Definition 7 defines an equivalence relation on $\Gamma$ for every $L \in \mathbb{N}$. The operator $H$ is said to have *finite local complexity* if the set of equivalence classes is finite for all $L$.

We also need to define a set of evaluation functions that allow the algorithm to make use of this additional structure. It would be sufficient to add some evaluation functions describing the size $R(L)$ of the smallest ball $B_{R(L)}(0)$ that contains representatives of all equivalence classes of patches of size $L$. But to keep the description of our algorithm closer to the way we implemented it for quasiperiodic Hamiltonians, we assume that the algorithm can directly access an enumeration of local patches and the Hamiltonians on them.

Let $\Omega_{\text{flc}}$ be the set of operators $H$ of finite local complexity. For each such operator, we can describe the structure of local patches by a combination of the following objects:

(1) A function $C_H : \mathbb{N} \to \mathbb{N}$ (counting the number $C_H(L)$ of local patches of size $L$).

(2) For every $L \in \mathbb{N}$ and $k \in \{1, \ldots, C_H(L)\}$, a number $Q_H(L, k) \in \mathbb{N}$ (counting the number of sites in the $k$th patch at scale $L$).

(3) For every $L \in \mathbb{N}$, $k \in \{1, \ldots, C_H(L)\}$, and $j \in \{1, \ldots, Q_H(L, k)\}$, a $d$-dimensional point $p_H(L, k, j)$, defining the relative position of the $j$th site in the $k$th patch.

(4) For every $L \in \mathbb{N}$ and $k \in \{1, \ldots, C_H(L)\}$, a $Q_H(L, k) \times Q_H(L, k)$-matrix $G_H(L, k)$ with entries in $\mathcal{L}(\mathcal{H})$.

Such that the following is fulfilled: If $L \in \mathbb{N}$ and $x \in \Gamma$, there is a $k \in \{1, \ldots, C_H(L)\}$ such that

(i) We have $|\Gamma \cap B_L(x)| = Q_H(L, k)$.

(ii) There is an enumeration $(\tilde{e}_j)_{j=1,\ldots,Q_H(L,k)}$ of $\Gamma \cap B_L(x)$ and there are $Q_H(L, k)$ unitary operators $U_j \in \mathcal{U}(\mathcal{H})$, $j = 1, \ldots, Q_H(L, k)$, such that

(a) For all $j = 1, \ldots, Q_H(L, k)$, we have $\tilde{e}_j - x = p_H(L, k, j)$.

(b) For all $i, j \in \{1, \ldots, Q_H(L, k)\}^2$, we have

$$U_i^* H_{ij} U_j = G_H(L, k)_{ij},$$

where $H_{ij}$ refers to the matrix entries (hoppings) of $H$ between $\tilde{e}_i$ and $\tilde{e}_j$.

Based on this, we can define the set of evaluation functions in $\Lambda_{\mathrm{flc}}$, which are functions $\Omega \to \mathbb{R}$, by basically interchanging indices and arguments of the functions above. For example, for every $L \in \mathbb{N}$ we can define an evaluation function

$$f_L^C(H) = C(L_H).$$

We can further let

$$f_{L,k}^Q(H) = \begin{cases} Q_H(L,k) & \text{if } k \leqslant C_H(L) \\ 0 & \text{otherwise} \end{cases}$$

for all $L, k \in \mathbb{N}$. We have defined the evaluation functions for $k > C_H(L)$ to be zero since the number of evaluation functions can obviously not depend on $H$. We can similarly define evaluation functions describing $p_H$ and $G_H$ with the appropriate number of indices. The union of all these functions defines the set $\Lambda_{\mathrm{flc}}$. With these definitions, we can state the following theorem.

*Theorem 3.* The computational problem $(\Omega_{\mathrm{flc}}, \Lambda_{\mathrm{flc}}, (\mathcal{M}, d), \Xi)$ is in $\Delta_1^A$.

A detailed proof of this theorem will be given in a future publication. Basically, one can combine the upper bound on the distance to the spectrum from [12] with the computable lower bound we provide here. The pertinent theorem on the upper bound from [12, Supplementary Material, Theorem 3] can be formulated as follows:

*Theorem 4 ([12]).* Let $A \in \Omega_2$ and let $\Gamma_n^{\mathrm{up}}(A), E^{\mathrm{up}}(n)$ be computed using the algorithm in [12] with size parameter $n$. Then $\Gamma_n^{\mathrm{up}}(A) \to \mathrm{Spec}(A)$ and $E^{\mathrm{up}}(n) \to 0$ as $n \to \infty$ and $\Gamma_n^{\mathrm{up}}(n)$ is contained in the $E^{\mathrm{up}}(n)$ neighbourhood of $\mathrm{Spec}(A)$. Moreover, $\Gamma_n$ can be implemented using finitely many arithmetic operations and comparisons on the matrix elements of $A$.

Using the algorithm in this article, we can also give the following statement on a computable lower bound for operators of finite local complexity:

*Theorem 5.* For the computational problem $(\Omega_{\mathrm{flc}}, \Lambda_{\mathrm{flc}}, (\mathcal{M}, d), \Xi)$, there exists an algorithm computing a spectral approximation $\Gamma_n^{\mathrm{low}}(H)$ and an error estimate $E_n^{\mathrm{low}}$ such that $\mathrm{Spec}(H)$ is contained in an $E_n^{\mathrm{low}}$ neighbourhood of $\Gamma_n^{\mathrm{low}}$.

These two theorems show that the spectral problem in our setting lies in $\Sigma_1^A$ (Theorem 4) and $\Pi_1^A$ (Theorem 5). Since the intersection $\Sigma_1^A \cap \Pi_1^A = \Delta_1^A$, the problem $(\Omega_{\mathrm{flc}}, \Lambda_{\mathrm{flc}}, (\mathcal{M}, d), \Xi)$ is in $\Delta_1^A$, that is, two-sided error control in Hausdorff distance is possible.

The proof of Theorem 5 is based on the following result, a partial inverse implication of the one contained in Theorem 1.

*Theorem 6.* Let $H$ be an operator on a uniformly discrete set $\Gamma \subseteq \mathbb{R}^d$ with finite hopping length $m \in \mathbb{R}$. Then for every $\delta > 0$ there exists an $\epsilon > 0$ and an $L \in \mathbb{N}$ such that $H$ is locally $\epsilon$-bulk gapped at scale $L$ for all energies $\lambda$ where the distance to the bulk spectrum $d(\lambda, \mathrm{Spec}(H)) > \delta$.

The tuple $(\epsilon, L)$ can be computed explicitly and depends only on $\|H\|_{\mathrm{op}}$, on $m$ and on $\Gamma$. The proof of Theorem 6, which will be presented in a future publication, relies on a discrete version of the well-known Combes-Thomas estimates [52].


[1] D. R. Hofstadter, Energy levels and wave functions of Bloch electrons in rational and irrational magnetic fields, Phys. Rev. B **14**, 2239 (1976).

[2] J. Bellissard and B. Simon, Cantor spectrum for the almost Mathieu equation, J. Funct. Anal. **48**, 408 (1982).

[3] A. Avila and S. Jitomirskaya, The ten martini problem, Ann. Math. **170**, 303 (2009).

[4] S. Becker, R. Han, and S. Jitomirskaya, Cantor spectrum of graphene in magnetic fields, Invent. Math. **218**, 979 (2019).

[5] C. Sire, Electronic spectrum of a 2d quasi-crystal related to the octagonal quasi-periodic tiling, Europhys. Lett. **10**, 483 (1989).

[6] C. Sire and J. Bellissard, Renormalization group for the octagonal quasi-periodic tiling, Europhys. Lett. **11**, 439 (1990).

[7] V. G. Benza and C. Sire, Band spectrum of the octagonal quasicrystal: Finite measure, gaps, and chaos, Phys. Rev. B **44**, 10343 (1991).

[8] M. E. Zoorob, M. D. B. Charlton, G. J. Parker, J. J. Baumberg, and M. C. Netti, Complete photonic bandgaps in 12-fold symmetric quasicrystals, Nature (London) **404**, 740 (2000).

[9] W. Man, M. Megens, P. J. Steinhardt, and P. M. Chaikin, Experimental measurement of the photonic properties of icosahedral quasicrystals, Nature (London) **436**, 993 (2005).

[10] J.-N. Fuchs and J. Vidal, Hofstadter butterfly of a quasicrystal, Phys. Rev. B **94**, 205437 (2016).

[11] T. A. Loring, Bulk spectrum and K-theory for infinite-area topological quasicrystals, J. Math. Phys. **60**, 081903 (2019).

[12] M. J. Colbrook, B. Roman, and A. C. Hansen, How to Compute Spectra with Error Control, Phys. Rev. Lett. **122**, 250201 (2019).

[13] L. N. Trefethen and M. Embree, *Spectra and Pseudospectra* (Princeton University Press, Princeton, 2020)

[14] M. A. Bandres, M. C. Rechtsman, and M. Segev, Topological Photonic Quasicrystals: Fractal Topological Spectrum and Protected Transport, Phys. Rev. X **6**, 011016 (2016).

[15] J. Kellendonk and E. Prodan, Bulkboundary correspondence for Sturmian Kohmoto-like models, Ann. Henri Poincaré **20**, 2039 (2019).

[16] O. Zilberberg, Topology in quasicrystals, Opt. Mater. Express **11**, 1143 (2021).

[17] M. Duneau, Approximants of quasiperiodic structures generated by the inflation mapping, J. Phys. A: Math. Gen. **22**, 4549 (1989).

[18] H. Tsunetsugu, T. Fujiwara, K. Ueda, and T. Tokihiro, Electronic properties of the Penrose lattice. I. Energy spectrum and wave functions, Phys. Rev. B **43**, 8879 (1991).

[19] E. Prodan, Quantum transport in disordered systems under magnetic fields: A study based on operator algebras, Appl. Math. Res. Express **2013**, 176 (2013).

[20] S. Beckus, J. Bellissard, and G. De Nittis, Spectral continuity for aperiodic quantum systems I. General theory, J. Funct. Anal. **275**, 2917 (2018).

[21] S. Beckus, J. Bellissard, and H. Cornean, Hölder continuity of the spectra for aperiodic Hamiltonians, Ann. Henri Poincaré **20**, 3603 (2019).

[22] T. A. Loring and H. Schulz-Baldes, The spectral localizer for even index pairings, J. Noncommut. Geom. **14**, 1 (2020).

[23] E. B. Davies, Spectral pollution, IMA J. Numer. Anal. **24**, 417 (2004).

[24] X. S. Li, An Overview of SuperLU: Algorithms, implementation, and user interface, ACM Trans. Math. Softw. **31**, 302 (2005).
[25] J. C. Lagarias, Geometric models for quasicrystals I. Delone sets of finite type, Discrete Comput. Geom. **21**, 161 (1999).
[26] M. Baake and R. V. Moody, Diffractive point sets with entropy, J. Phys. A: Math. Gen. **31**, 9023 (1998).
[27] J. C. Lagarias and P. A. B. Pleasants, Local complexity of Delone sets and crystallinity, Can. Math. Bull. **45**, 634 (2002).
[28] V. Elser, Comment on "Quasicrystals: A New Class of Ordered Structures", Phys. Rev. Lett. **54**, 1730 (1985).
[29] R. V. Moody, Model sets: A survey, in *From Quasicrystals to More Complex Systems* (Springer, New York, 2000), pp. 145–166.
[30] N. G. de Bruijn, Algebraic theory of Penroses non-periodic tilings of the plane, Indagationes Mathematicae (Proceedings) **84**, 39 (1981).
[31] C. Janot, *Quasicrystals: A Primer*, 2nd ed. (Oxford University Press, Oxford, 2012).
[32] R. Ammann, B. Grünbaum, and G. C. Shephard, Aperiodic tiles, Discrete Comput. Geom. **8**, 1 (1992).
[33] F. P. M. Beenker, *Algebraic Theory of Non-periodic Tilings of the Plane by Two Simple Building Blocks: A Square and a Rhombus*, Technical Report 82-WSK-04 (Eindhoven University of Technology, 1982).
[34] A. Julien, Complexity and cohomology for cut-and-projection tilings, Ergod. Theory Dyn. Syst. **30**, 489 (2010).
[35] I. C. Fulga, D. I. Pikulin, and T. A. Loring, Aperiodic Weak Topological Superconductors, Phys. Rev. Lett. **116**, 257002 (2016).
[36] J. Vidal and R. Mosseri, Quasiperiodic tilings in a magnetic field, J. Non-Cryst. Solids **334–335**, 130 (2004).
[37] D.-T. Tran, A. Dauphin, N. Goldman, and P. Gaspard, Topological Hofstadter insulators in a two-dimensional quasicrystal, Phys. Rev. B **91**, 085125 (2015).
[38] J.-N. Fuchs, R. Mosseri, and J. Vidal, Landau levels in quasicrystals, Phys. Rev. B **98**, 165427 (2018).
[39] M. J. Colbrook and A. C. Hansen, The foundations of spectral computations via the solvability complexity index hierarchy, J. Eur. Math. Soc. (to be published), arXiv:1908.09592.
[40] J. Ben-Artzi, A. C. Hansen, O. Nevanlinna, and M. Seidel, Computing spectra – on the solvability complexity index hierarchy and towers of algorithms, arXiv:1508.03280.
[41] Y. Saad, *Numerical Methods for Large Eigenvalue Problems: Revised Edition* (SIAM, Philadelphia, 2011).
[42] M. Kohmoto, L. P. Kadanoff, and C. Tang, Localization Problem in One Dimension: Mapping and Escape, Phys. Rev. Lett. **50**, 1870 (1983).
[43] S. Ostlund, R. Pandit, D. Rand, H. J. Schellnhuber, and E. D. Siggia, One-Dimensional Schrödinger Equation with an Almost Periodic Potential, Phys. Rev. Lett. **50**, 1873 (1983).
[44] S. Even-Dar Mandel and R. Lifshitz, Electronic energy spectra of square and cubic Fibonacci quasicrystals, Philos. Mag. **88**, 2261 (2008).
[45] A. Jagannathan, The Fibonacci quasicrystal: Case study of hidden dimensions and multifractality, Rev. Mod. Phys. **93**, 045001 (2021).
[46] D. Damanik, M. Embree, and A. Gorodetski, Spectral properties of Schrödinger operators arising in the study of quasicrystals, in *Mathematics of Aperiodic Order* (Springer, New York, 2015), pp. 307–370.
[47] D. Damanik, J. Fillman, and A. Gorodetski, Continuum Schrödinger operators associated with aperiodic subshifts, Ann. Henri Poincaré **15**, 1123 (2014).
[48] D. Lenz, C. Seifert, and P. Stollmann, Zero measure Cantor spectra for continuum one-dimensional quasicrystals, J. Diff. Equ. **256**, 1905 (2014).
[49] M. Casdagli, Symbolic dynamics for the renormalization map of a quasiperiodic Schrödinger equation, Commun. Math. Phys. **107**, 295 (1986).
[50] A. Sütő, The spectrum of a quasiperiodic Schrödinger operator, Commun. Math. Phys. **111**, 409 (1987).
[51] A. Hansen, On the solvability complexity index, the n-pseudospectrum and approximations of spectra of operators, J. Am. Math. Soc. **24**, 81 (2011).
[52] J.-M. Combes and L. Thomas, Asymptotic behaviour of eigenfunctions for multiparticle Schrödinger operators, Commun. Math. Phys. **34**, 251 (1973).